



# Analysis of winter thermal comfort conditions: street scenarios using ENVI-met model

Sevgi Yılmaz<sup>1</sup> · Elif Akpınar Külekçi<sup>1</sup> · Başak Ertem Mutlu<sup>1</sup> · Işık Sezen<sup>1</sup>

Received: 4 August 2020 / Accepted: 4 December 2020 / Published online: 18 January 2021  
© The Author(s), under exclusive licence to Springer-Verlag GmbH, DE part of Springer Nature 2021

## Abstract

Rapid migration to cities and the increasing demand for housing negatively affect living areas. Furthermore, uncontrolled population growth, industrialization, urbanization, narrowing of urban areas, and expansion of cities cause physical boundaries. Urbanization growth and the cold climate restrict pedestrian mobility in the city. Therefore, hourly microclimate data of the city center streets were collected 1.5 m above ground level in the winter period of 2019–2020. Then, different landscape design scenarios on pedestrian roads were investigated extensively using the ENVI-met V.4.4.2 winter model to determine the outdoor thermal comfort level. The RayMan model was utilized to generate the sky view factor (SVF) and analyze the mean values of the microclimate data. The proposed landscape design scenarios were as follows; (1) hard-covered street, (2) complete street coverage with a canopy, (3) street coverage with a semi-canopy, (4) sage of a combination of different plant species (30% deciduous, 30% coniferous, 30% bush), and (5) usage of ornamental pools in streets. The time period when pedestrians used the outdoor space was taken into consideration in evaluating and interpreting the analysis results. The findings of this study generally indicated that the semi-open canopy design provided roads with high thermal comfort such that people can walk and cycle in winter time. In conclusion, the thermal comfort condition of a street design, which is important for achieving sustainable urbanization, can be changed by making appropriate plan decisions. The findings of this study will help improve the outdoor thermal comfort in the first stage of urban planning and landscape street design for more livable and effective cities. This study emphasizes that a multidisciplinary team should work together to establish a healthy, sustainable, and livable urbanized area with thermal comfort in the streets.

**Keywords** Outdoor thermal comfort · ENVI-met V.4.4.2 winter · Livable street · Pedestrian · Street scenarios

## Introduction

The United Nations Climate Change Conference focuses public attention on global climate change and environmental

protection. Studies are being made to prevent the gradual depletion of resources found in nature, which is the host of living and non-living beings. It is very important to produce sustainable and ecologically-based livable spaces and to do this with climate-oriented solutions. With these solutions, it is necessary to step into a sustainable future. Academic studies continue in this direction to solve the climatic and environmental problems of megacities (Foley et al. 2005; Huang et al. 2016; Chen et al. 2017; Smith et al. 2018; Xu et al. 2019; Xiong et al. 2020).

The density of 100 people per km<sup>2</sup> at the village and municipal level has been defined as the threshold for the definition of rural areas. Densely settled areas with a density of more than 500 people per km<sup>2</sup> and a population greater than 50,000; places with densities ranging from 500 to 100 people per km<sup>2</sup> and with a population of more than 50,000 are medium-densely settled regions; Places with a density of less than 100 people per km<sup>2</sup> and a population of less than 50,000 are

---

Responsible Editor: Marcus Schulz

✉ Elif Akpınar Külekçi  
eakpinar@atauni.edu.tr

Sevgi Yılmaz  
syilmaz\_68@hotmail.com; sevgiy@atauni.edu.tr

Başak Ertem Mutlu  
basakertem\_14@hotmail.com

Işık Sezen  
isiksezen@atauni.edu.tr

<sup>1</sup> Faculty of Architecture and Design, Department of Landscape Architecture, Atatürk University, 25240 Erzurum, Turkey

defined as low-density settled regions (Yoloğlu and Zorlu 2020). According to the OECD 2012, the large metropolitan area is a functional urban area with a population of 1.5 million or more, the metropolitan area with a population of 500,000 to 1.5 million, the medium-sized metropolitan area with a population of 200,000 to 500,000, and the small urban area with a population of 50,000 to 200,000. Accordingly, areas with a population of less than 50,000 are defined as rural areas (Yoloğlu and Zorlu 2020). In big cities, the air temperatures in both summer and winter are higher than those in surrounding rural areas. For medium-sized cities, central and rural areas differ by approximately 0.5–3.0 °C, with reasonable corresponding changes in the microclimate (Battista et al. 2019). The deterioration of the urban microclimate adversely affects the thermal comfort of city residents (Xu et al. 2017; Santamouris et al. 2018; Yilmaz et al. 2018a). Increasing urban green areas has recently been considered an effective solution to these problems (Nastos and Polychroni 2016; Morakinyo et al. 2018; Sosa et al. 2017; Xiao et al. 2018; Cocco et al. 2018).

It is known that urban geometry, which is one of the factors affecting the thermal comfort of the city, has an effect on outdoor microclimate parameters (Golany 1996). Microclimate is the atmospheric conditions of a certain area that differs from the larger area in the environment and is affected by the urban texture and urban development of the former area. Microclimate includes a number of parameters that reflect the climatic conditions of the focal region (Toy and Yilmaz 2010; Shareef and Abu-Hijleh 2020; Unger et al. 2020). Microclimate and outdoor thermal conditions are greatly affected by urban geometry and building configuration (Zanon and Verones 2013; Yilmaz et al. 2018b; Yilmaz et al. 2019).

Thermal environment of street canyons plays an important role in determining quality of urban physical environment. Thermal environment of a city varies depending on factors such as reflections of building facades (Xu et al. 2019), impervious surfaces (Chun and Guldmann 2014), vegetation (Imran et al. 2019), and water areas (Gunawardena et al. 2017). In addition, sky view factor (Dirksen et al. 2019), vertical growth, means of transport (Palme et al. 2016), population density, and height/width ratio (Bakarman and Chang 2015) are effective factors in heat generation in cities (Zhang et al. 2020). General comfort determined by air temperature, humidity, wind speed and radiation is closely related to the perception and preference of the way people use the outdoors (Hwang et al. 2011; Huang et al. 2015; Nastos and Polychroni 2016; Maniatis et al. 2020).

In recent years, many studies have been conducted on outdoor thermal comfort, which is directly related to human activity. The open space that comprises the urban environment differs from interior spaces; a person standing on a street experiences fluctuations in thermal stimuli, which affect their

thermal comfort, due to radiation in two ways. The first is the shortwave radiation that is emitted from the extremely hot surface of the sun and is often called sunlight. The second is the longwave radiation emitted by the atmosphere and the low-temperature terrestrial surfaces in our surrounding environment (Ma et al. 2019).

By filtering and minimizing shortwave radiation, trees can reduce air and surface temperatures and help improve thermal comfort (Lee et al. 2014; Lee et al. 2020). Evergreen trees regulate the climate by reducing the wind speed in the environment and partly blocking the effect of direct sunlight on surfaces (Irmak et al. 2018; Zhang et al. 2018). Deciduous trees, on the other hand, increase thermal comfort by providing shadows during warm seasons and by letting sunlight pass through during cold seasons (Perini et al. 2018). Trees affect microclimatic conditions by controlling air flows, reducing wind speed, and changing wind direction (Perini et al. 2018). They also reduce air and surface temperatures by evaporation, shading, and filtering of direct sunlight (Morakinyo et al. 2017).

Another component that affects the thermal comfort of pedestrian roads or streets is the Sky View Factor (SVF). This varies depending on the ratio between the width of a street and the floor heights of the buildings along that street. SVF is an important quantitative indicator that defines circular geometric shape (Unger 2009; Chen et al. 2012; Algeciras et al. 2016). In terms of landscape architecture, SVF can also be used as an editing index to reflect the landscape morphology of a street canyon (Li et al. 2020).

Studies on the thermal environment of street canyons are mostly performed under certain local climatic conditions, and more studies are conducted in warm, humid climates (Bowler et al. 2010; Gómez-Baggethun and Barton 2013; De Abreu-Harbach et al. 2015). There are very few studies in cold climates (Bourbia and Boucheriba 2010; Park et al. 2012; Ma et al. 2019; Yilmaz et al. 2021). In a study for hot summer and cold winter days, Xiong et al. (2020) determined that the microclimate and thermal comfort of a Chinese garden can generally be improved by increasing the water coverage, reducing the building coverage, and optimizing the tree coverage.

Pedestrian-friendly walking paths, sidewalks, and street designs are important in for urban spaces (Yilmaz et al. 2016). In these places, where people spend time, studies are performed in the context of improving thermal comfort. For this purpose, scholars have investigated how thermal comfort is influenced by the leaf characteristics of trees on roads, sidewalks, or streets (Pearlmutter et al. 2007); street orientation (Krüger et al. 2010; Cao et al. 2015; Mutlu et al. 2018); sky view factor (SVF) on pedestrian roads (Zhang et al. 2017); presence of urban vegetation (Morakinyo et al. 2018; Yilmaz et al. 2021); and shade coating materials (Erell et al. 2014). Sidewalks and their coating materials also affect thermal comfort in walkable pedestrian roads (Yang and Lin 2016).

Scenarios produced in this model can be subjected to thermal comfort analysis (Taleb and Abu-Hijleh 2013; Perini and Magliocco 2014; Taleghani et al. 2015; Unger et al. 2020).

The physiologically equivalent temperature (PET) is a thermal index that shows the heat balance of the human body (Höppe 1993). PET results are reliable in open-air urban areas in both cold and hot stress climate zones (Monam and Rückert 2013; Barakat et al. 2017; Hu et al. 2019). Because these parameters show the same temperatures, they are similar to human energy stress balancing results (Blazejczyk et al. 2012; Chatzidimitriou and Axarli 2017; Abaas 2020).

According to the classifications made by Köppen and Geiger on climate, the city of Erzurum is in group of the coldest climates. This classification study is one of the most widely used analyses in the world (Köppen 1918; Köppen and Geiger 1954; Öztürk et al. 2017), the most widely used classification worldwide, created by Wladimir Petrovich Köppen in 1918 and developed by Rudolf Geiger. Taş Mağazalar Street, which is intensely used by the public, is a road with a variety of commercial stores. This is because this street is the place that the local people most commonly use. Successful outdoor environment of the pedestrian road can significantly contribute to the humans' activity and living.

The aim of this study is to determine the thermal comfort conditions required for people to go out in winter season and to set an example with this study in the historical "Taş Mağazalar Street," the only pedestrian road in Erzurum. In the research, solution proposals will be given in order to ensure that a maximum level of thermal comfort is provided for the public, especially in the winter season. The necessary methods, which will be followed when designing suitable pedestrian roads for thermal comfort in Erzurum and allowing the individuals to use the pedestrian roads without being disturbed by the weather conditions, have been contemplated. In this context, different scenarios have been examined for the selected road and analyzed using thermal comfort indexes.

## Material and method

Erzurum, a historical and a cultural city, is located in the Eastern Anatolia region of Turkey. The study area, the Taş Mağazalar Street, is the oldest and the pedestrian road in terms of history and is the only street in the city (Fig. 1). The Taş Mağazalar Street is a heavily used area during summer and winter time in Erzurum, one of the coldest winter cities in Turkey. The street is in the city center of Yakutiye District (39° 54' 30.7548" latitude and 41° 16' 41.4300" longitude) and oriented in the northwest–southeast direction. The width of the street including sidewalks is about 10 m, and there are only a few stores, mostly jewelry stores, along it. This street was closed to traffic by Erzurum Municipality in 2009 and then designed as a pedestrian road. It is the only pedestrian

road in the city that is closed to traffic. It is a lively street where people shops generally for traditional weddings. The use of the street is quite limited since the icicles formed on the roofs in winter and the ice on the ground makes walking difficult for pedestrians. Before the pedestrian path was declared, the street that was used much less in winter was mobilized after the pedestrian path was declared and the floor covering was made.

However, there is still no desired level of use during the winter months. The floor of the pedestrian road is usually andesite stone covered and hard ground. After the pedestrian path was declared by the local government, wooden seating benches, seasonal plant crates, a small ornamental pond, and *Pyrus calleryana* were planted. In the middle of the pedestrian road, sometimes street vendors sell. There is no shaded place in the shops.

## Field measurement on site and meteorological data

One-year meteorological data for 2019 from the meteorological station in the city center were used in thermal comfort analysis. In the ENVI-met V.4.4.2 winter computer model, winter months were preferred, especially for use in the scenario analyses; measurements were made in January and February. Within the scope of the study, 24-h meteorological parameters were measured from the street on February 25, 2019, and February 25, 2020. Data were recorded with Ycom-Kmn 305 model temperature and humidity meter mounted 1.5 m above the floor of one of the shops along Taş Mağazalar (Fig. 3). This device obtained the ambient air temperature ( $T_a$ , °C), relative humidity (RH—%), wind speed (m/s), wind direction, and cloud (Octas) data. Then, 24-h temperature data on February 25, 2019, were also acquired from the nearest weather station for temperature comparison. A Davis Vantage Pro2 device was used to measure the meteorological data (Fig. 2). This device, which was installed at the city center at 1.5 m from the ground, has the same features as the device used by the General Directorate of Meteorology.

The SVF was calculated to determine the street canyon. For this purpose, measurements were obtained with a fisheye lens attached to a Nikon D5200 camera. While these measurements were being made, shots were captured from the middle of the road, toward north, and toward the sky at a height of 1.1 m from the ground. The measuring point is given in Fig. 3. The shots obtained were analyzed in the RayMan Pro 2 computer model. SVF values between 0 and 1 were obtained in these analyses, where 1 indicated 100% sky visibility.

Information about the hourly meteorological data used in the ENVI-met V.4.4.2 winter computer model in the thermal comfort analyses and prepared scenarios are given in Tables 1 and 2. In this model, the scenarios can be analyzed using 24-h meteorological data (Bruse 2000). Winter was preferred for

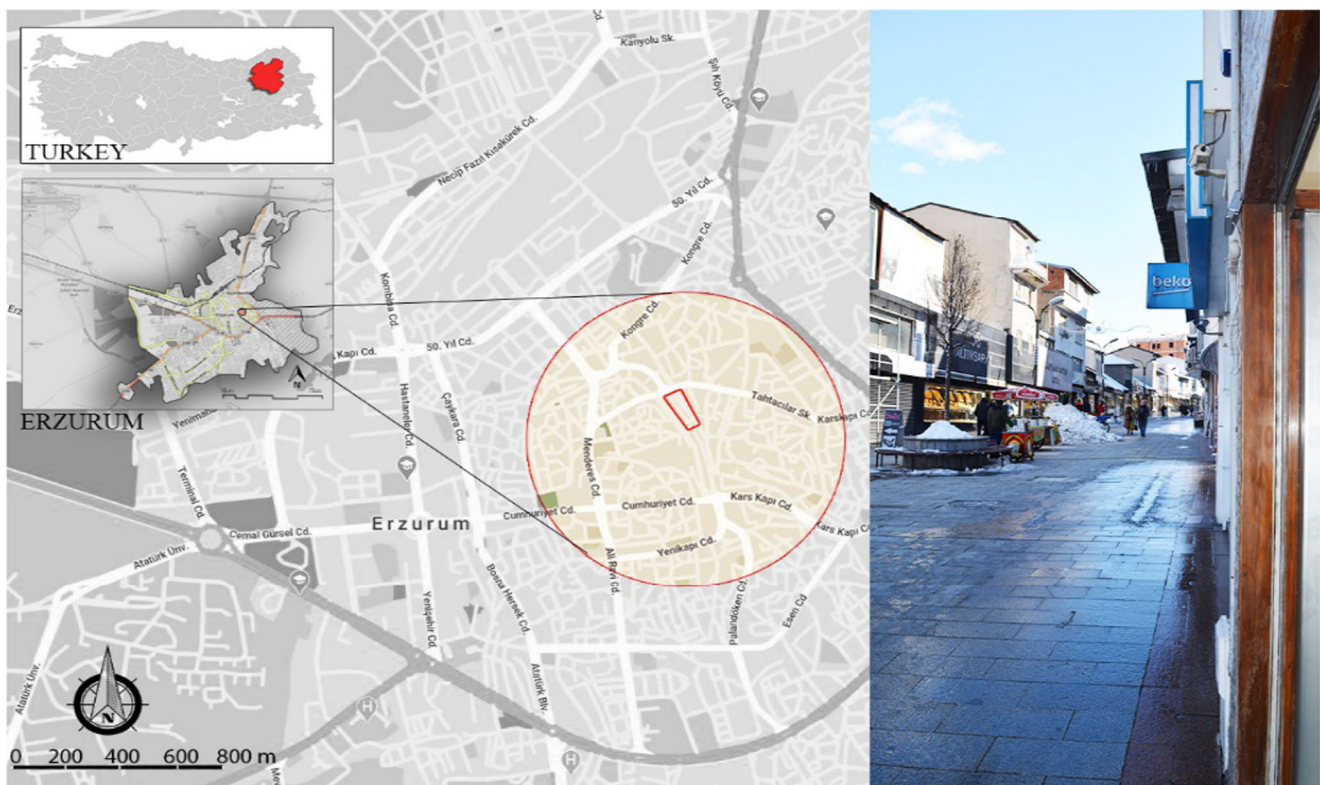


**Fig. 1** The location of the study area in Erzurum—“Taş Mağazalar Street”

the analysis of these scenarios in ENVI-met. Wind measurements were made at approximately 1.5 height above ground level on this street.

Erzurum province has very low wind averages due to the city center and the annual average wind speed is 2.7 m/s. Looking at the average values for many years, the months with the lowest wind speed are December (2.1 m/s), January (2.1 m/s), and February (2.3 m/s), respectively (MGM 2020).

### ENVI-met V4.4.2 winter soft model

The ENVI-met program is a high-resolution microclimate model developed by Bruse (2000) to simulate ground, facade, vegetation, and weather relationships in urban areas. The ENVI-met software used has a very high sensitivity in estimating the outdoor thermal environment. The ENVI-met model is often used to find factors affecting street canyon, urban heat island, and outdoor thermal comfort and to analyze the scenarios offered. Different computer models and indexes are used in determining outdoor thermal comfort. In total, 77% of ENVI-met studies were published during the last 5 years (Tsoka et al. 2018). ENVI-met model sizes are limited to 50\*50\*30 (X, Y, Z) grids. It has a typical horizontal resolution between 0.5 and 5 m. It simulates air temperature ( $T_a$ —°C), relative humidity (RH—%), wind speed (m/s) and direction, and long radiation waves. The data used in ENVI-met for the scenarios we analyzed are given in Table 3. The research is

based on the three-dimensional ENVI-met model (Bruse 2000, 2020), which simulates microclimate conditions in urban environments with a high spatial and temporal resolution. This numerical modeling was preferred because of its affordable cost and its ability to easily compare the urban climate with the city elements used.

The characteristics of the plants in the scenarios used in the study area are given in Table 3. Considering the plants used, since the program is limited, the plants existing in the program were used. The properties of the plants could not be changed. The model is suited for this task, but it needs to be developed. Because model simulates pavement, canopy materials, and a kind of tree that may not exist in the real world. Therefore, in future studies, we should consider different landscape design scenarios (Liu et al. 2018; Ma et al. 2019). For now, it is a disadvantage, but the model continues to be developed.

Plants of the modeled area were selected from the database of the software model, which match the existing plants and species obtained during the field measurements as described below: Fig. 4.

### ENVI-met 4.4.2 winter model accuracy analysis

The accuracy of the simulation performance was also examined using difference measures of the model evaluation, which have been used by Qaid et al. 2016; Battista et al. 2016; Acero



Fig. 2 Davis Vantage Pro2 measurement device

and Arrizabalaga 2018; and Yilmaz et al. 2021. These measures include Willmott (1982)’s index of agreement ( $d$ ). The simulation results are regarded as reliable if these measures are close to the following requirements:  $d \rightarrow 1$ . In this study, the simulations made and the accuracy of the measurements taken were analyzed. The accuracy of the model was checked by calculating agreement index ( $d$ ) (Fig. 6). Analyses were made according to a certain formula with this verification method developed by Willmott (1982). Agreement index ( $d$ ) is a descriptive measure that indicates to what level the simulated values are error-free. It has a value between 0 and 1. Here, a value of 1 means absolute agreement indicating that the simulated values ( $s$ ) are equal to the observed values ( $o$ ). Agreement index ( $d$ ), which is the first indicator, takes a value between 0 and 1 and the closer this value is to 1, the more accuracy is achieved (Acero and Arrizabalaga 2018).

Accuracy analysis of this model was made for the winter months of 2019–2020. Air temperature plays a major role in determining the performance of accuracy analysis. In order to evaluate the winter performance of the model in 2019 and 2020, 7 statistical parameters were used in the calibration of the observed ( $O$ ) and predicted ( $P$ ) data for both years. Statistical parameters used: fit index ( $d$ ) is the coefficient of determination ( $R^2$ ), mean bias error (MBE), mean absolute error (MAE) are listed as. The mean bias error (MBE) shows whether the values from the model are higher or lower than the observed data. The mean absolute error (MAE) is the same as the MBE indicator but takes into account the absolute difference between predicted and observed values (Battista et al.2016). The MBE/MAE value must be between 0 and 1. If this value is 1 or close to 1, it shows the accuracy of the model. Studies generally emphasize the benefit of fit index ( $d$ ). Values vary between 0 and 1 for the two statistical measurements evaluated. If the values are close to 1 and 1, it

shows that most of the data are fit and close to the regression line. But if the values are close to 0 and 0, it shows that most of the variation data are far from the regression line, and the data fit is low. The values of fit index ( $d$ ) and determination coefficient ( $R^2$ ) in the analyses made in the figure are high, which represents the harmony values of the data (Qaid and Ossen 2015). However, the distribution points do not fit the line, showing distribution in the positive and negative directions of the regression line. Points in this distribution are acceptable as they show the difference between observed ( $O$ ) and predicted ( $P$ ) data. However, the difference between the predicted ( $P$ ) and the observed ( $O$ ) data is expected and occurs in many studies based on the simulation model including the ENVI-met model. In this context, higher  $R^2$  value represents the differences between the observed ( $O$ ) data and the predicted ( $P$ ) data are smaller and unbiased. Unbiased values, known as the fitted values, are not systematically too high or too low. On the other hand, a higher value of  $d$  indicates that the degree of error in the prediction data is very low. The observed ( $O$ ) and the predicted ( $P$ ) air temperature in Fig. 5 indicates the  $R^2$  for 2019 (0.85) and  $R^2$  for 2020 (0.87) (Fig. 6).

In the analyses for the winter months of 2019 and 2020, the coefficient of determination ( $R^2$ ) is very close to 1, which shows that they are statistically significant. In addition, the fit index ( $d$ ) was determined as 0.74 for 2019 and 0.87 for 2020. Since the values in the fit index are close to 1, the performance of the model is quite good. These results show that the software has been well verified and the work can be run with these software outputs.

Meanings of Abbreviations in the formula (Battista et al. 2016):

- $d$  Index of agreement [–]
- MAE Mean absolute error [–]
- MBE Mean bias error [–]
- $N_D$  Number of analyzed data [–]
- $\bar{O}$  Mean of the observed variable
- $O_j$  Observed variables for each instant  $j$
- $P_j$  Model-predicted variables for each instant  $j$

$$d = 1 - \frac{\sum_{j=1}^{N_D} [(P_j - \bar{O}) - (O_j - \bar{O})]^2}{\sum_{j=1}^{N_D} (|P_j - \bar{O}| + |O_j - \bar{O}|)^2}$$

$$MBE = \frac{\sum_{j=1}^{N_D} (P_j - O_j)}{N_D}$$

$$MAE = \frac{\sum_{j=1}^{N_D} |P_j - O_j|}{N_D}$$

**Fig. 3** Study area measurement point and devices for measuring air temperature, SVF, and TROTEC BA16 anemometer wind speed measurement device



When the observed and simulated air temperature for 2019 are evaluated,  $d$  value is 0.74 (Table 4).

When the observed and simulated air temperatures of 2020 are evaluated,  $d$  value is 0.87 (Table 5).

### The physiologically equivalent temperature

The PET values were obtained by using RayMan Pro 2 to determine the thermal comfort. One-year meteorological data for 2019 from the meteorological station established in the city center were used to obtain the PET values. In this

program, the standard value is based on the dimensions of a European man who is 1.75 m in height, 75 kg in weight, and is wearing a jacket (Matzarakis et al. 1999). The coordinates and altitude of the study area were entered. The values resulting from the analysis are in °C, and the evaluation was performed according to Table 6. This graphic shows the human thermal comfort situation in the cities. PET contains all relevant meteorological parameters such as air temperature, wind, relative humidity, and radiation. Besides, PET also includes personal factors such as people's activity level, the clothes they wear, and age (Höppe 1999). PET provides an accurate

**Table 1** Meteorological data of February 25, 2019 (winter)

Time	Air temperature (°C)	Relative humidity (%)	Wind speed (m/s)	Wind direction
00:00	-4.4	86	0	---
1:00	-5.1	84	0	---
2:00	-5.8	87	0	---
3:00	-6.2	85	0	---
4:00	-6.3	85	0	---
5:00	-7.4	88	0	---
6:00	-7.7	87	0	---
7:00	-7.4	88	0	---
8:00	-5.9	79	0	ESE
9:00	-3.9	69	0	ESE
10:00	-1.5	69	0	SE
11:00	-0.8	70	0	ESE
12:00	-1.9	69	0.4	ESE
13:00	-1.5	71	0	ESE
14:00	-0.9	69	0	NW
15:00	-1.1	73	0	NW
16:00	-1.4	76	0	WNW
17:00	-2.1	79	0	WNW
18:00	-3.3	81	0	---
19:00	-3.7	83	0	S
20:00	-4.3	84	0	ESE
21:00	-5.1	84	0	NW
22:00	-4.2	84	0	---
23:00	-4.3	84	0	---

**Table 2** Meteorological data from February 25, 2020 (winter)

Time	Air temperature (°C)	Relative humidity (%)	Wind speed (m/s)	Wind direction
00:00	-9.0	68	2.2	N
1:00	-9.0	69	2.7	SW
2:00	-9.1	72	3.8	SW
3:00	-10.1	75	3.9	SW
4:00	-10.0	75	4.3	SSW
5:00	-11.0	76	4.5	SSW
6:00	-11.0	77	4.5	SSW
7:00	-11.0	75	4.3	WNW
8:00	-10.8	72	4.1	WNW
9:00	-9.7	70	3.7	WNW
10:00	-8.0	65	3.8	WNW
11:00	-6.5	62	3.8	WNW
12:00	-4.6	56	3.8	WNW
13:00	-3.2	55	4.7	WNW
14:00	-1.2	53	4.7	WNW
15:00	-1.4	52	4.8	WNW
16:00	-1.6	56	4.7	WNW
17:00	-2.0	58	4.6	WNW
18:00	-3.2	61	4.1	NW
19:00	-5.2	62	3.1	NW
20:00	-6.1	65	3.0	N
21:00	-7.3	67	2.7	N
22:00	-8.0	67	1.4	N
23:00	-9.2	68	1.3	N

**Table 3** Data used in the ENVI-met V.4.4.2 winter program

Location	Erzurum City Center
Climate type	Mountain ecosystem
Simulation period	Values
Total simulation duration	24 h for 1 landscape design
Spatial resolution	1 m×2 m×1 m
Domain size (number of grid cell)	X=45, Y=100, Z=30
Model rotation	33°
Date	25.02.2019/ 25.02.2020
Basic meteorological input	Unshaded
Wind speed (m/s)	2019 (0.1)/2020 (3.7)
Wind direction (°)	(2019—112.5°/2020—292.5°)
Air temperature for 24 h	+ (simple forced)
Relative humidity for 24 h	+ (simple forced)
Lowest air temperature (°C)/h	2019 (−7.7/06:00) 2020 (−11.0/06:00)
Highest air temperature (°C)/h	2019 (−0.8/11:00) 2020 (−1.2/14:00)
Lowest humidity	2019 (69%/10:00) 2020 (52%/15:00)
Highest humidity	2019 (88%/05:00) 2020 (77%/06:00)
Sky condition	Clear
Information of designs	
Hard-covered surface	
Completely canopy	
Semi canopy	
Different plant species	10 deciduous plant + 10 coniferous plant + 10 bush plant
Ornamental pool	

representation of human thermal comfort using the easy-to-understand climate index. PET is widely used in many studies and its applications in different outdoor environments have been studied in detail (Mayer and Höpfe 1987; Gulyás et al. 2006; Potchter et al. 2018; Jamei and Rajagopalan 2019).

### Designed proposed scenarios for street design

Five proposed scenarios were created considering factors that affect the thermal comfort on streets. These scenarios and their features are in Fig. 7.

- **Proposed scenario 1:** The floor was completely covered with hard pavement material and had no plants.
- **Proposed scenario 2:** The top of the street was completely covered with canopy materials.
- **Proposed scenario 3:** The street was half-open, half-closed. A canopy was installed on the wall of the shops, and an opening was left in the middle.
- **Proposed scenario 4:** This scenario was based on the use of plants grown widely in the city. Ten deciduous trees

(*Betula sp. L.*), ten coniferous trees (*Pinus sylvestris L./Scots pine*), and ten bushes (30% deciduous, 30% coniferous, 30% bush) were considered.

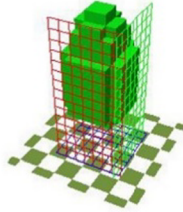
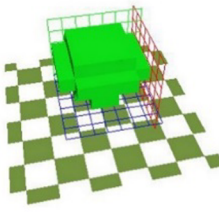
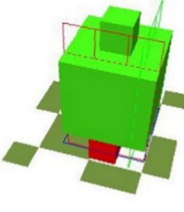
- **Proposed scenario 5:** A 4-m-wide ornamental pool was designed extending from the beginning of the street to determine the effect of water. The depth of this place, which is considered as an ornamental pool, is designed as 15–20 cm.

### Results

In this study, the analysis of alternative scenarios for livable, walkable thermal comfortable pedestrian roads was done with ENVI-met V.4.4.2 winter. In this place, which is the only pedestrian way of Erzurum, SVF, and micro-climate measurements were made. The SVF value affecting the thermal comfort was analyzed for this street. The SVF obtained from the middle of the street at 1.1 m above ground was 0.752 (Fig. 8).



**Fig. 4** Data used in the ENVI-met V.4.4.2 winter program for plants

Deciduous plant	Coniferous plant	Bush
Pine (ID: 0000C2)	<i>Betula pendula</i> (ID: 0000B7)	Cylindric, small trunk, sparse, small (ID: 010SSS)
Height (m): 15.00 Width (m): 7.00 Cells: 7*7*15	Height (m): 6.00 Width (m): 7.00 Cells: 7*7*6	Height (m): 5.00 Width (m): 3.00 Cells: 3*3*5
		
<p><b>General Information</b></p> <p>ID: 0000C2 Color: <span style="color: green;">■</span></p> <p>Name: Pine</p> <p>Alternative Name: Scots Pine</p> <p><b>Plant geometry</b></p> <p>Height (m): 15.00</p> <p>Width (m): 7.00</p> <p>Cells: 7 x 7 x 15</p> <p>Resolution (m): 1.00</p> <p><b>Basic properties</b></p> <p>CO2 fixation type: C3-Plant</p> <p>Leaf type: Conifer Leaves</p> <p>Foliage Shortwave Albedo: 0.18</p> <p>Foliage Shortwave Transmittance: 0.30</p> <p><b>Advanced Properties</b></p> <p>Leaf Weight [g/m<sup>2</sup>]: 100.00</p> <p>Isoprene Capacity: 12.00</p> <p><b>Root Settings</b></p> <p>Depth of roots (m): 1.20 <span>Edit root data...</span></p> <p>Diameter of roots (m): 6.00</p> <p><input type="checkbox"/> Display Root Zone</p>	<p><b>General Information</b></p> <p>ID: 0000B7 Color: <span style="color: green;">■</span></p> <p>Name: Betula Pendula</p> <p>Alternative Name: Silver Birch</p> <p><b>Plant geometry</b></p> <p>Height (m): 6.00</p> <p>Width (m): 7.00</p> <p>Cells: 7 x 7 x 6</p> <p>Resolution (m): 1.00</p> <p><b>Basic properties</b></p> <p>CO2 fixation type: C3-Plant</p> <p>Leaf type: Deciduous Leaves</p> <p>Foliage Shortwave Albedo: 0.18</p> <p>Foliage Shortwave Transmittance: 0.30</p> <p><b>Advanced Properties</b></p> <p>Leaf Weight [g/m<sup>2</sup>]: 100.00</p> <p>Isoprene Capacity: 12.00</p> <p><b>Root Settings</b></p> <p>Depth of roots (m): 1.40 <span>Edit root data...</span></p> <p>Diameter of roots (m): 10.00</p> <p><input type="checkbox"/> Display Root Zone</p>	<p><b>General Information</b></p> <p>ID: 010SSS Color: <span style="color: black;">■</span></p> <p>Name: Cylindric, small trunk, sparse,</p> <p>Alternative Name: (none)</p> <p><b>Plant geometry</b></p> <p>Height (m): 5.00</p> <p>Width (m): 3.00</p> <p>Cells: 3 x 3 x 5</p> <p>Resolution (m): 1.00</p> <p><b>Basic properties</b></p> <p>CO2 fixation type: C3-Plant</p> <p>Leaf type: Deciduous Leaves</p> <p>Foliage Shortwave Albedo: 0.18</p> <p>Foliage Shortwave Transmittance: 0.30</p> <p><b>Advanced Properties</b></p> <p>Leaf Weight [g/m<sup>2</sup>]: 100.00</p> <p>Isoprene Capacity: 12.00</p> <p><b>Root Settings</b></p> <p>Depth of roots (m): 3.00 <span>Edit root data...</span></p> <p>Diameter of roots (m): 3.00</p> <p><input type="checkbox"/> Display Root Zone</p>

**Fig. 5** Observed and predicted air temperature for 2019

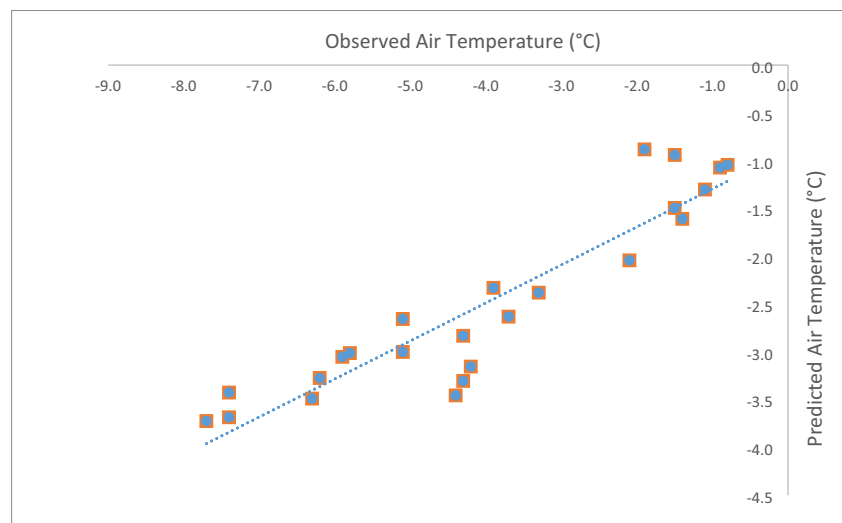
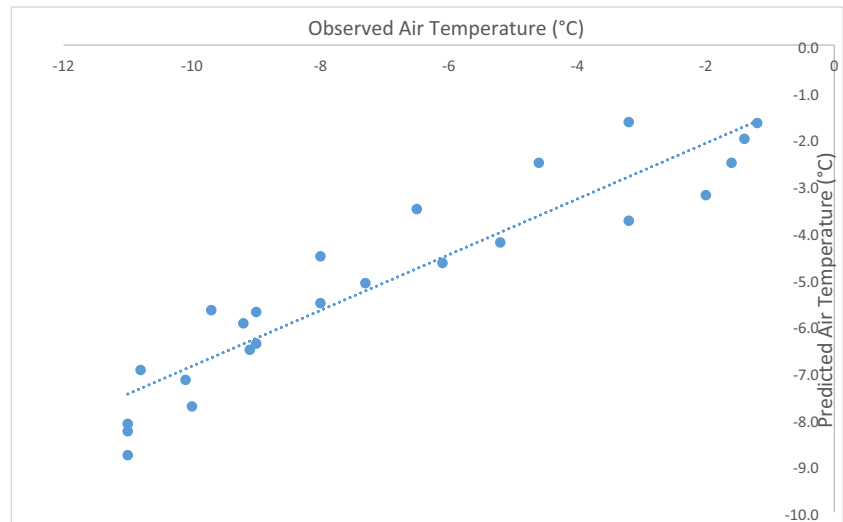


**Fig. 6** Observed and predicted air temperature for 2020



This value indicates that the street has a wide canyon feature and clear sky visibility. The reason for the high rate of sky view factor is that there are no tall buildings that will block the view angle. According to the SVF value obtained, the sky visibility of this pedestrian path is clear. The height of the

floors of the adjacent buildings on the right and left of the pedestrian road generally has a single and several three-story buildings. On this pedestrian path, on average, the ratio of floor height to road width, that is, canyon value (Street Aspect ratio) was determined as 0.4 (H/W). The average

**Table 4** Evaluation of measured and simulated temperatures in 2019

Date	Time	Observed air temperature (°C)	Simulated air temperature (°C)	Difference	Difference square	Index of agreement ( <i>d</i> )
25.02.2019	00:00	-4.4	-3.5	0.9441	0.89132481	0.741761967
25.02.2019	01:00	-5.1	-2.7	2.4436	5.97118096	
25.02.2019	02:00	-5.8	-3.0	2.787	7.767369	
25.02.2019	03:00	-6.2	-3.3	2.9264	8.56381696	
25.02.2019	04:00	-6.3	-3.5	2.8107	7.90003449	
25.02.2019	05:00	-7.4	-3.7	3.7153	13.80345409	
25.02.2019	06:00	-7.7	-3.7	3.9761	15.80937121	
25.02.2019	07:00	-7.4	-3.4	3.974	15.792676	
25.02.2019	08:00	-5.9	-3.1	2.8477	8.10939529	
25.02.2019	09:00	-3.9	-2.3	1.5696	2.46364416	
25.02.2019	10:00	-1.5	-1.5	0.0055	3.025E-05	
25.02.2019	11:00	-0.8	-1.0	-0.2436	0.05934096	
25.02.2019	12:00	-1.9	-0.9	1.01817	1.036670149	
25.02.2019	13:00	-1.5	-0.9	0.55982	0.313398432	
25.02.2019	14:00	-0.9	-1.1	-0.1722	0.02965284	
25.02.2019	15:00	-1.1	-1.3	-0.2015	0.04060225	
25.02.2019	16:00	-1.4	-1.6	-0.2086	0.04351396	
25.02.2019	17:00	-2.1	-2.0	0.0571	0.00326041	
25.02.2019	18:00	-3.3	-2.4	0.9192	0.84492864	
25.02.2019	19:00	-3.7	-2.6	1.0682	1.14105124	
25.02.2019	20:00	-4.3	-2.8	1.4678	2.15443684	
25.02.2019	21:00	-5.1	-3.0	2.0987	4.40454169	
25.02.2019	22:00	-4.2	-3.2	1.0456	1.09327936	
25.02.2019	23:00	-4.3	-3.3	0.9958	0.99161764	

**Table 5** Evaluation of measured and simulated temperatures in 2020

Date	Time	Observed air temperature (°C)	Simulated air temperature (°C)	Difference	Difference square	Index of agreement ( <i>d</i> )
25.02.2019	00:00	-9.0	-6.4	2.6108	6.81627664	0.870895527
25.02.2019	01:00	-9.0	-5.7	3.2868	10.80305424	
25.02.2019	02:00	-9.1	-6.5	2.5773	6.64247529	
25.02.2019	03:00	-10.1	-7.2	2.9335	8.60542225	
25.02.2019	04:00	-10.0	-7.7	2.2655	5.13249025	
25.02.2019	05:00	-11.0	-8.3	2.7333	7.47092889	
25.02.2019	06:00	-11.0	-8.8	2.2222	4.93817284	
25.02.2019	07:00	-11.0	-8.1	2.8933	8.37118489	
25.02.2019	08:00	-10.8	-7.0	3.8449	14.78325601	
25.02.2019	09:00	-9.7	-5.7	4.0257	16.20626049	
25.02.2019	10:00	-8.0	-4.5	3.478	12.096484	
25.02.2019	11:00	-6.5	-3.5	2.9897	8.93830609	
25.02.2019	12:00	-4.6	-2.5	2.0808	4.32972864	
25.02.2019	13:00	-3.2	-1.6	1.5517	2.40777289	
25.02.2019	14:00	-1.2	-1.7	-0.4678	0.21883684	
25.02.2019	15:00	-1.4	-2.0	-0.6067	0.36808489	
25.02.2019	16:00	-1.6	-2.5	-0.9206	0.84750436	
25.02.2019	17:00	-2.0	-3.2	-12.118	1.46845924	
25.02.2019	18:00	-3.2	-3.8	-0.56	0.3136	
25.02.2019	19:00	-5.2	-4.2	0.9751	0.95082001	
25.02.2019	20:00	-6.1	-4.7	1.4361	2.06238321	
25.02.2019	21:00	-7.3	-5.1	2.2044	4.85937936	
25.02.2019	22:00	-8.0	-5.5	2.4766	6.13354756	
25.02.2019	23:00	-9.2	-6.0	3.2441	10.52418481	

height of the buildings on both sides of the street is taken and proportioned to the existing road width. As a matter of fact, according to a study, the best street canyon rates to determine the sunlight were determined. Accordingly, it was stated that this ratio should be planned in the form of narrow canyon streets larger than ( $Y/G \geq 0.5$ ) in hot climatic regions and that this ratio should include wide canyon street features less than

( $Y/G \leq 0.5$ ) in cold climatic regions (Shishegar 2013; Bendida et al. 2019).

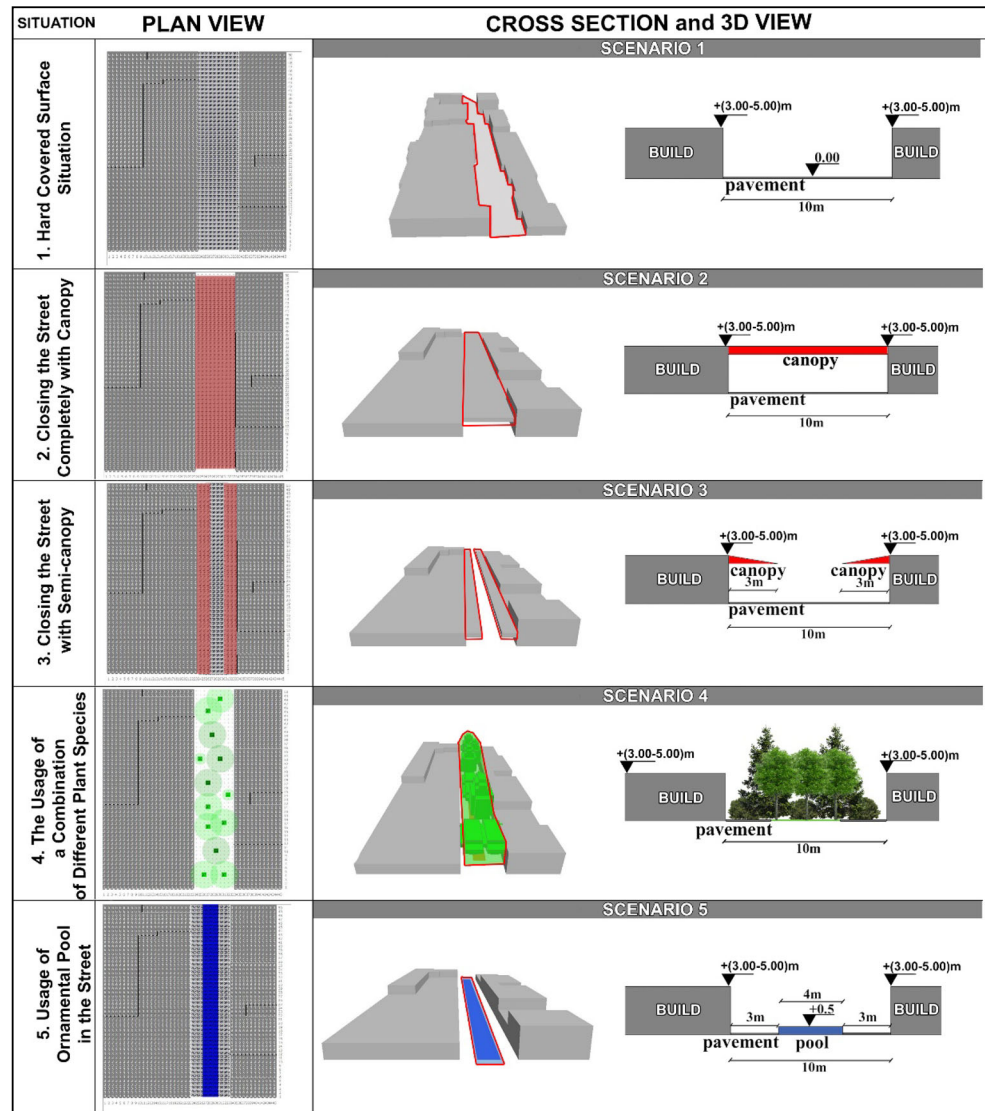
**Climate in the study area and the physiologically equivalent temperature analysis**

Erzurum is among the coldest cities of Turkey. Winter months are quite cold in Erzurum, which is categorized as “cold winter city” according to Köppen climate criteria (Köppen 1918). It is important for the inhabitants of Erzurum to go out and wander, especially during the winter months, and to ensure the thermal comfort of this pedestrian axis. The people of the city will be able to use the pedestrian axle more frequently and for a longer period of time. For this purpose, the PET chart was prepared using the data of 2019. PET analysis is mostly used in outdoor thermal comfort studies (Golasi et al. 2016; Potchter et al. 2018). The ability to spend time outdoors comfortably without sweating excessively or feeling extreme cold will increase the availability of places. Additional measurements and analyses should be conducted to obtain and improve the standards of accessible and livable cities. The values of the meteorology device installed at the city center and

**Table 6** PET value ranges (Matzarakis et al. 1999)

PET	Thermal sensitivity	Grade of physiological stress
4.0 °C>	Very cold	Extreme cold stress
4.1–8.0 °C	Cold	Strong cold stress
8.1–13.0 °C	Cool	Moderate cold stress
13.1–18.0 °C	Slightly cool	Slightly cold stress
18.1–23.0 °C	Neutral (comfortable)	No thermal stress
23.1–29.0 °C	Slightly warm	Slightly heat stress
29.1–35.0 °C	Warm	Moderate heat stress
35.1–41.0 °C	Hot	Strong heat stress
>41.0 °C	Very hot	Extreme heat stress

**Fig. 7** Proposed street scenarios features



recorded hourly data were used to obtain the PET values in this study. This device was installed at a height of 1.5 m from the ground because, according to European standards, microclimatic parameters affect people at this level.

PET (Matzarakis et al. 1999) by definition: “It has been defined as a thermal index that serves to evaluate the thermal component of different climates. In addition to being based on physiological evaluations, it uses a universally known unit of measure ( $^{\circ}\text{C}$ ), which is important for those less familiar with current human biometeorological terminology. One of its most important features is that it enables the determination of the thermal component of microclimates in urban environments.” Figure 9 shows the PET graph prepared using the 2019 meteorological data in terms of thermal comfort assessment. In the figure, blue indicates cold temperatures, and red indicates heat. This figure reveals that a colder weather will be more effective for outdoor thermal comfort in the city. The comfortable

days were mostly in the summer months, and heat stress was mostly experienced in August. In Erzurum City, long winter months and poor pavement conditions caused by ice make walking difficult.

Table 7 shows the maximum, minimum, and average PET values obtained in the PET analysis using the 2019 meteorological data. PET values for 2019 in Fig. 12 are classified according to the PET ranges in Table 6. In 2019 PET chart, it was calculated by obtaining air temperature, humidity, wind speed, and cloudiness data. The values in Table 7 include the average, maximum, and minimum values of monthly values. According to Table 7, June, July, and August are seen as the PET value, that is, the best thermal comfort. According to the PET values in Table 6, the best thermal value range is 18.1–23.0  $^{\circ}\text{C}$ . Therefore, the winter months were generally under the influence of cold stress. In November, December, January, and February, the PET values were below 4.0  $^{\circ}\text{C}$ , and extreme cold stress was experienced. The minimum PET value (–

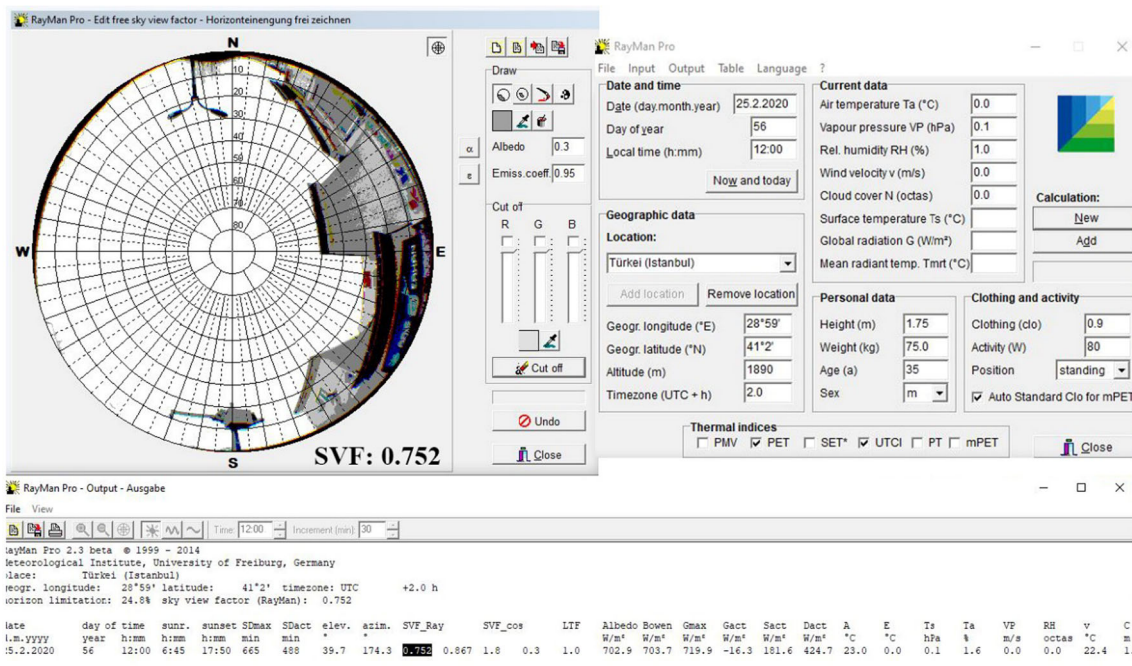


Fig. 8 Taş Mağazalar Pedestrian Street SVF analysis

26.4 °C) was experienced in January. The maximum PET value was 42.1 °C, which was identified in August.

**ENVI-met analysis of scenarios**

The five proposed scenarios created to determine the thermal comfort values and design pedestrian-friendly roads were analyzed with the ENVI-met V.4.4.2 winter computer model. In

this context, we attempted to determine which street design has the best thermal comfort. Thus, 24-h data from the street on February 25, 2019, and February 25, 2020, were analyzed. The scenarios created were analyzed for the dates taken. The area of trees, buildings, canopy, and hard-covered surface used in the scenarios created is proportioned according to the total area of 45 m\*100 m in m<sup>2</sup>, and it is calculated how many % it covers.

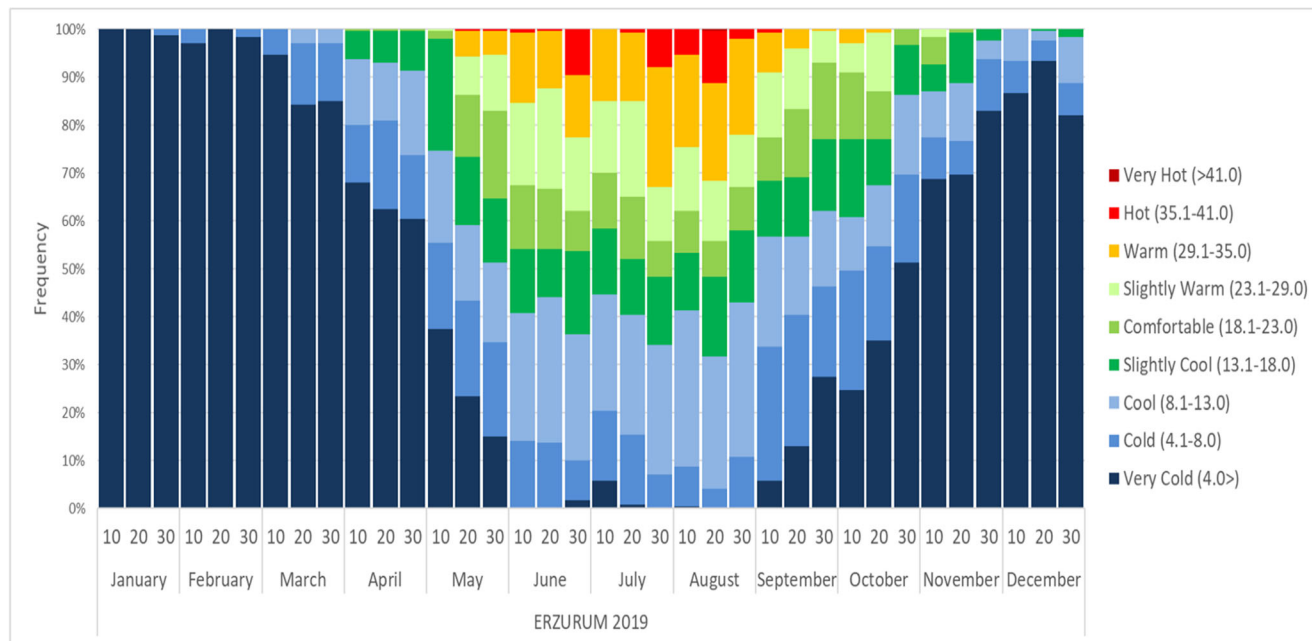


Fig. 9 PET graphic of Erzurum City for 2019

**Table 7** PET analysis data for 2019

Months		Air temperature (°C)	Humidity (%)	Wind speed (m/s)	Cloudiness	PET (°C)
January	Min	-19.4	47	0.0	0.0	-26.4
	Max	5.2	99	5.1	10.0	5.1
	Mean	-5.7	73	0.9	5.4	-9.9
February	Min	-16.9	45	5.7	0.0	-23.4
	Max	2.7	99	0.0	10.0	6.4
	Mean	-5.3	78	0.7	4.5	-8.7
March	Min	-13.1	31	0.0	0.0	-20.5
	Max	8.7	99	7.0	10.0	10.6
	Mean	-1.3	74	1.3	5.0	-4.7
April	Min	-2.4	20	0.0	0.0	-9.2
	Max	16.2	99	6.0	8.8	19.8
	Mean	4.4	70	1.3	5.9	2.0
May	Min	0.6	2	0.0	0.0	-5.6
	Max	25.6	99	6.7	8.8	39.9
	Mean	12.6	54	1.3	3.8	11.1
June	Min	5.9	13	0.0	0.0	0.0
	Max	29.4	99	6.2	8.8	39.3
	Mean	18.5	48	1.3	3.7	18.2
July	Min	5.4	11	0.0	0.0	-0.4
	Max	34.7	95	6.1	8.8	40.3
	Mean	20.0	43	1.7	2.2	18.7
August	Min	9.3	7	0.0	0.0	3.8
	Max	33.6	99	5.1	8.8	41.2
	Mean	20.8	41	1.6	1.8	19.5
September	Min	-0.1	10	0.0	0.0	-5.3
	Max	26.1	91	7.2	8.8	35.1
	Mean	14.8	48	1.5	2.6	12.5
October	Min	-0.9	7	0.0	0.0	-5.3
	Max	24.0	98	6.7	8.8	34.0
	Mean	11.1	52	0.9	2.8	8.3
November	Min	-8.0	13	0.0	0.0	-14.2
	Max	16.5	99	5.1	10.0	28.5
	Mean	2.3	56	0.5	1.8	-0.8
December	Min	-11.0	32	0.0	0.0	-18.1
	Max	8.0	99	4.6	10.0	15.3
	Mean	-2.0	80	0.5	5.1	-4.2

**Proposed scenario 1** The 3D image used in the program for this scenario is given in Fig. 10. In this design, the street is completely covered with a hard surface, and cut andesite stone is used as the floor covering. Total working area is 4,500 (45 m \* 100 m) m<sup>2</sup>. In the first scenario, the area covered by the buildings is 3500 (35 m \* 100 m) m<sup>2</sup>, and the area covered by the hard floor is (10 m \* 100 m) 1000 m<sup>2</sup>. When compared to the total area, the rate of building was 77.7%, and the floor rate was 22.3%. For the street completely covered with a hard surface, the ENVI-met analysis for February 25, 2019, revealed a minimum temperature of -2.5 °C and a maximum

of -1.1 °C. On February 25, 2020, the minimum was -2.1 °C, and the maximum was -0.7 °C.

**Proposed scenario 2** In this scenario, the street is completely covered with a canopy material. The visual 3D image of this scenario is given in Fig. 11. In this street scenario, a covering material that does not overwhelm snow and rain is considered. Road safety consisting of snow and ice will be ensured, especially in winter. Out of these scenarios, in the second scenario, unlike the area in the 1st scenario, the top canopy was used. Looking at the total area of 4500 (45 m \* 100 m) m<sup>2</sup>, the top

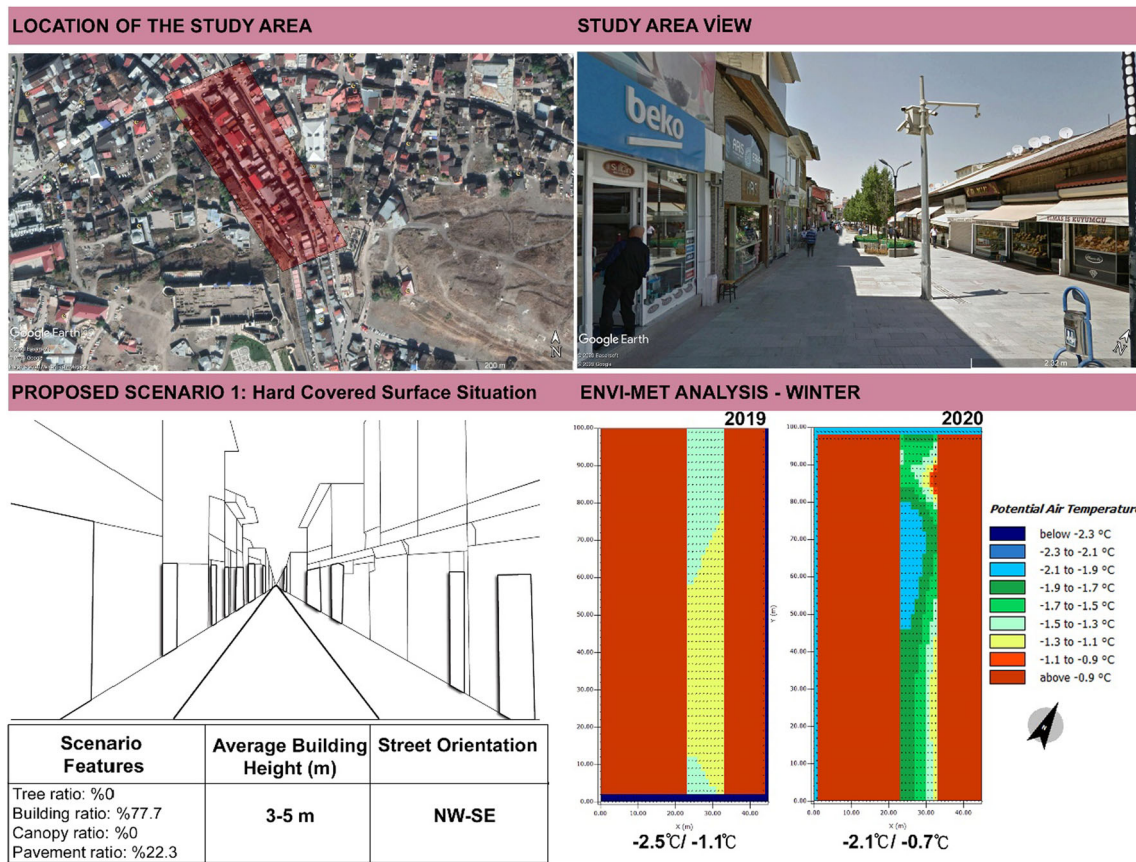


Fig. 10 Proposed scenario 1 (hard-material-covered surface) perspective view

canopy is 1000 (10 m \* 100 m) m<sup>2</sup> and has a ratio of 22.3%. In this scenario, the street is completely covered and a tent effect is created. When the proposed complete canopy cover scenario was analyzed in ENVI-met V.4.4.2 winter, the temperatures were at least -2.0 °C and at most 15.9 °C for February 25, 2019. The analysis was repeated twice, but the value remained the same. Looking at the minimum and maximum values in the scenario; it was observed that there was a deviation in the analysis and especially the maximum value was found to be much higher than it should have been. Therefore, the scenario has been modeled again and analyzed for the same climatic conditions. The same values were obtained. So, the results were evaluated by ignoring the high maximum values. It was thought that this high value was due to the program error. As stated in previous studies, it is known that the program has some deficiencies and is still being developed (Bruse 2020), although it is one of the most widely used programs in modeling climate scenarios (Tsoka et al. 2018). However, there are some limitations in use of the ENVI-met Model (Zhang et al. 2018).

**Proposed scenario 3** The 3D image for the half-covered, half-open design of the top of the street is shown in Fig. 12. In this scenario, it is designed to have some clearance above the pedestrian path. It was thought to provide an advantage on

rainy days as well. In the third scenario, one of the proposed scenarios, a semi-open canopy is used. When looking at a total area of 4500 (45 m \* 100 m) m<sup>2</sup>, the top canopy is 500 (5 m \* 100 m) m<sup>2</sup>, and has a ratio of 11.15%. The spaces left in this scenario will also help with ventilation. When this scenario was analyzed in the ENVI-met V.4.4.2 winter, the temperatures were a minimum of -2.5 °C and a maximum of -0.6 °C for February 25, 2019. For February 25, 2020, the minimum was -2.1 °C, and the maximum was -0.8 °C.

**Proposed scenario 4** This scenario uses different plants that are widely grown in Erzurum and adapted to the climate of the place. In the vegetative design of the street, 10 deciduous trees (*Betula sp. L.*), 10 coniferous trees (*Pinus sylvestris L.*), and 10 bushes were considered. The 3D view of this scenario (mixed plants) is given in Fig. 13. While choosing the trees, natural plants in the region were preferred. *Betula sp. L.*, which adapts specially to winter conditions and sheds its leaves in winter, is used. *Pinus sylvestris L.* was also analyzed as the coniferous plant, which was green during the winter months. A coniferous shrub type is intended to be used under coniferous and leafy trees. In the scenario 4, one of the proposed scenarios, plants design is used. Considering the total area of 4500 (45 m \* 100 m) m<sup>2</sup>, the plants area is 700 (7 m \* 100 m) m<sup>2</sup>, and has a rate of 15.55%. Since the plants design



Fig. 11 Proposed scenario 2 (complete canopy) perspective view

was used in the area, the ratio of hard ground has changed. The hard floor ratio is 300 (3 m \* 100 m) m<sup>2</sup> and has a ratio of approximately 6.8%. When the scenario with mixed plant was analyzed in ENVI-met V.4.4.2 winter, the temperatures were a minimum of -2.5 °C and a maximum of -1.1 °C for February 25, 2019. For February 25, 2020, the minimum was -2.3 °C, and the maximum was -0.7 °C.

**Proposed scenario 5** In this scenario, a 4-meter-wide ornamental pool passes right in the middle of the street. The 3D image prepared for the fifth scenario of the study area is given in Fig. 14. An ornamental pool was also designed to analyze the effect of water on thermal comfort. The pool extending from the beginning to the end of the street is designed to be in the shape of a channel. In the 5th scenario, one of the proposed scenarios, an ornamental pool is used. Considering the total area of 4500 (45 m \* 100 m) m<sup>2</sup>, the ornamental pool is 400 (4 m \* 100 m) m<sup>2</sup>, and has a ratio of 8.8%. Since the ornamental pool was used in the area, the rate of hard ground has changed. The hard floor ratio is 600 (6 m \* 100 m) m<sup>2</sup> and has a ratio of approximately 13.5%. Since this is an ornamental pool, a depth of 15–20 cm is considered. Here, it was aimed to analyze the effect of water on thermal comfort. When the proposed ornamental pool design was analyzed in ENVI-

met V.4.4.2 winter, the temperatures were at least -2.5 °C and at most -1.4 °C for February 25, 2019. For February 25, 2020, the minimum was -2.3 °C, and the maximum was -1.1 °C.

### Comparison of proposed scenario analysis

In this study, it has been tried to find out which design is more advantageous in thermal comfort in the pedestrian road. It is thought that people will use safe and thermal comfort areas in winter. For this purpose, designs were compared according to the ENVI-met V.4.4.2 winter version analysis of the data obtained as a result of the February 2019–2020 measurements.

The ENVI-met analysis of all the scenarios of the study, conducted on February 25, 2019, and February 25, 2020, is given in Fig. 15. The potential air temperature for 2020 is warmer by 0.4 °C on average than that of 2019. The hottest air temperature was found in scenario 2, where the top of the street is fully covered. The average temperature was 8.3 °C warmer in 2019 compared with that in 2020. Meanwhile, 2020 was on average 0.1 °C warmer than 2019 in scenario 3, where the top of the study area is half-covered. For the mixed design in scenario 4, 2020 was 0.3 °C warmer on average compared with 2019. In scenario 5, which features an



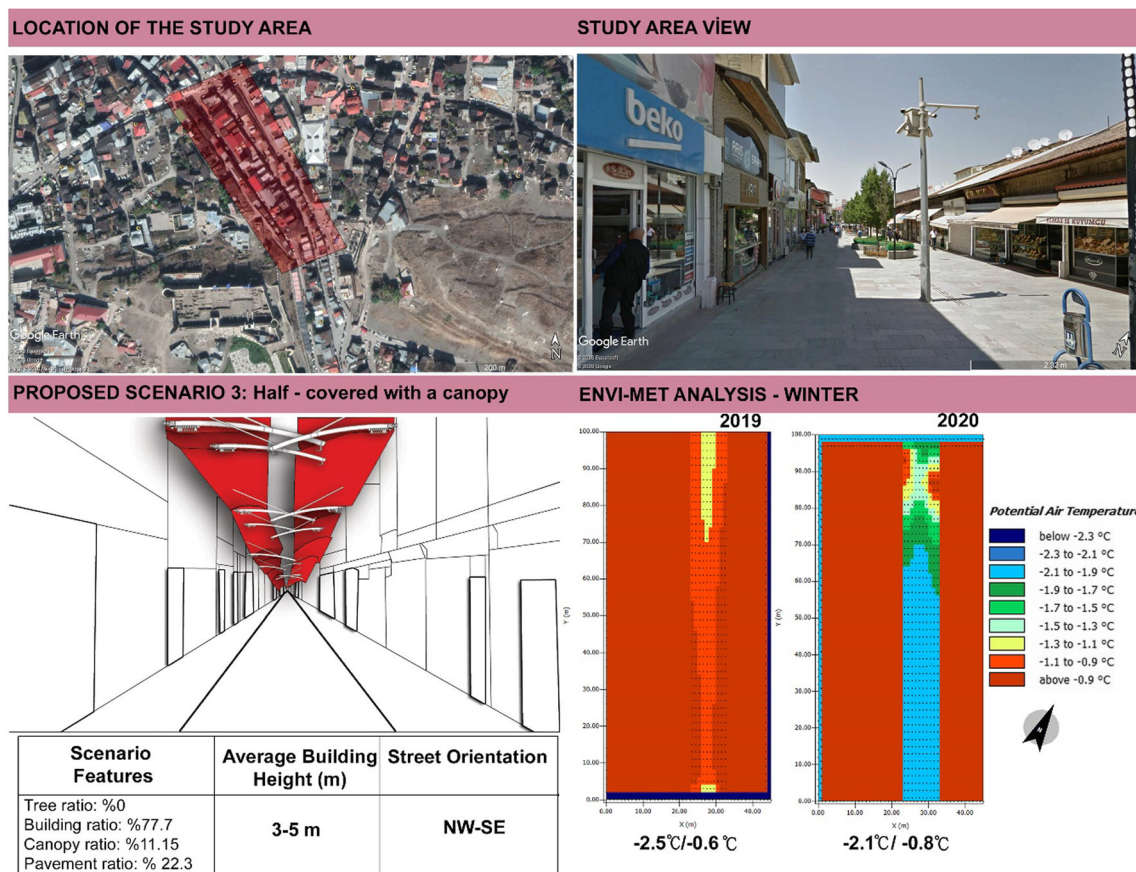


Fig. 12 Analysis of proposed scenario 3 designed as a semi-closed canopy

ornamental pool, the year 2020 was 0.3 °C hotter than 2019. In all the analyses except for scenario 2, the average temperatures in 2020 were warmer than those in 2019 (Fig. 15).

The suggested scenarios were evaluated according to the first scenario, where the street is covered with a hard surface. In 2019, the complete canopy scenario temperature increased the average temperature by 8.8 °C, while the semi-canopy scenario increased the temperature by 0.2 °C. There was no change in the air temperature range of the mixed plant scenario compared to the hard-covered surface scenario. When the ornamental pool proposal is examined, it was found that it reduces the air temperature by 0.2 °C according to the hard-covered surface scenario. In the analysis for 2020, the complete canopy scenario’s air temperature was higher by 0.1 °C compared with that of the hard-material-covered surface scenario. The semi-canopy and mixed-plants scenarios cooled the air temperature by 0.1 °C. The scenario with the ornamental pool cooled the air temperature by 0.3 °C (Fig. 16).

### Discussion

In this research, scenarios were designed for walkable pedestrian-friendly street designs, and analyses were

conducted using thermal comfort indexes. In general, thermal comfort studies aim to reduce thermal stress and improve thermal comfort (Huang et al. 2015; Yilmaz et al. 2019). Cold months prevail in Erzurum City. Therefore, we aimed to find a solution that would enable people to go outdoors and use the streets in winter. The street chosen for this research has a historical background and is used by the people of the city intensively in the summer. Scenarios were modeled and analyzed to reduce the trouble of urban people in the streets during winter and improve their thermal comfort conditions. Previous studies have indicated that city dwellers encounter difficulties in using outdoor spaces in winter (Hwang et al. 2011; Park et al. 2012; Xiong et al. 2020). There are similar problems in Erzurum; there are fewer streets and less frequent strolls in the winter months. In this study, it has been observed that temperatures in 2020 had risen in comparison to 2019. It has also been mentioned in various other studies that climate change has been increasingly felt over the years (Smith et al. 2018; Xu et al. 2019; Xiong et al. 2020).

It is important to analyze the thermal comfort of this pedestrian road, which is used extensively by the people of the city, especially in the summer. Indeed, different studies have also examined the thermal comfort of streets (Xu et al. 2017; Santamouris et al. 2018). It has been observed that pedestrian

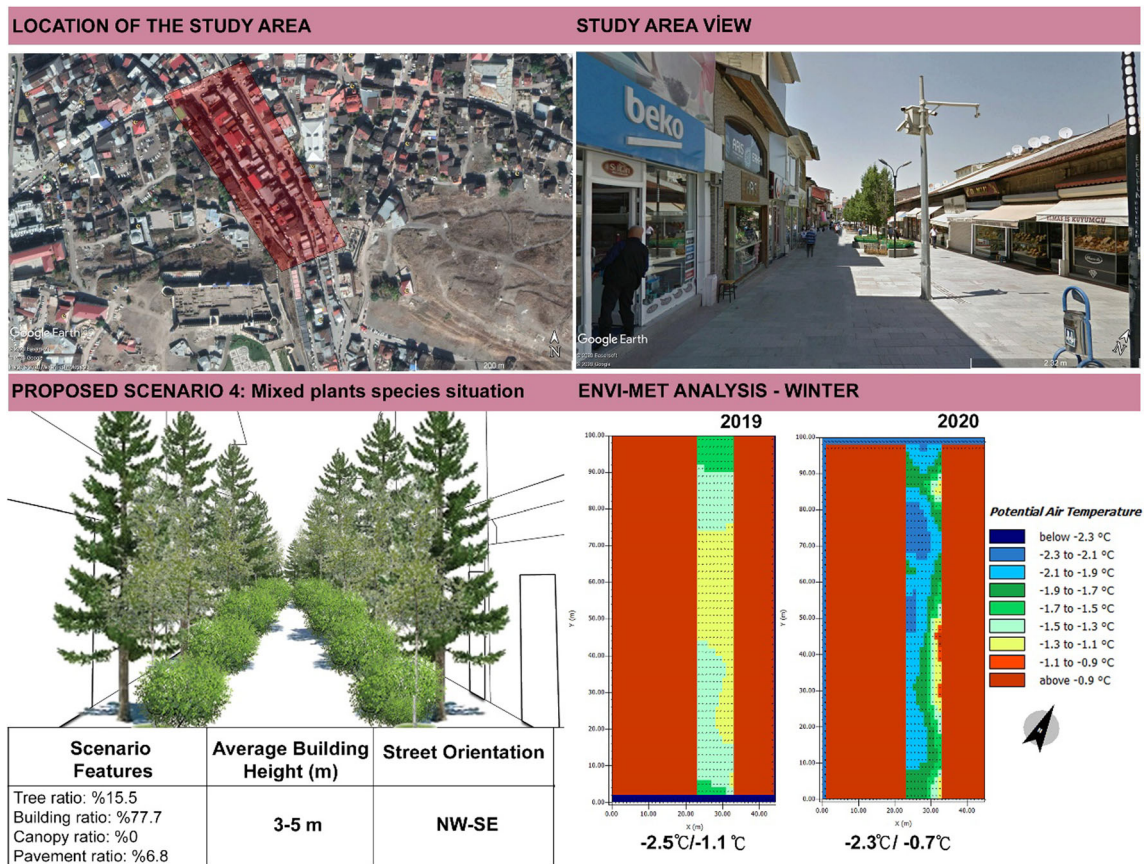


**Fig. 13** Proposed scenario 4 (mixed plants—30% deciduous, 30% coniferous, 30% bush) perspective view

roads surrounded by buildings are cooler than open areas. The shadow and wind circulation created by these structures may be effective in these spaces. During the winter months, ice lasts long on the pavements of the studied street. Therefore, its use in winter decreases slightly.

Considering the proposed scenarios, sheltered areas increase thermal comfort during the winter months. This was verified by the completely canopy scenario, where the temperature was higher by about 10.0 °C and 15.0 °C compared with those of the scenario with a completely hard-covered surface in 2019. In 2020, the completely canopy scenario was found to be 0.2 °C warmer than the area a completely hard-covered surface. The reason why the full-covered scenario increased to 15.9 °C in 2019 is that the wind speed was almost 0.0 in 2019 and the wind angle prevented the air flow in the covered area. There are also some limitations in the ENVI-met model. This result was evaluated by ignoring the high maximum values. It was thought that this high value was due to the program error. Meanwhile, ENVI-met is one of the most widely used models in studies of the impact of different landscape design scenario on thermal comfort environments, and it is an effective simulation model (Tsoka et al. 2018; Yilmaz et al. 2021).

Due to the lack of wind movement, the warmed air remained in the same environment and the ambient

temperature increased. This has led to the difference in air temperature between 2020 and 2019. The complete canopy will create a place protected from rain and wind. However, this temperature will increase, which is an important advantage for the winter months but will be disadvantageous in summer as it will cause heat stress. Thus, it is not appropriate to have a total canopy in all seasons.

The thermal comfort of the environment was better in the semi-open, semi-closed canopy system. The average minimum value of 2 years revealed that this scenario was 0.3 °C warmer than the hard-covered scenario. The semi-open, semi-closed scenario, which had a 0.2 °C average maximum value, was advantageous than the mixed-plants scenario. The plants' shading of this space and the sunlight filtration by the coniferous plants cooled the environment. Many studies have found that plants have a cooling effect (Morakinyo et al. 2018; Xiao et al. 2018; Coccolo et al. 2018). Cheung and Jim (2018) stated in their study that large trees in urban space cool the 3.9 °C environment. The positive contribution of the trees was found in other studies conducted during the winter months (Yilmaz et al. 2018c; Irmak et al. 2018). The aim is to design places where people can spend time in more thermally comfortable conditions in winter. However, these conditions are not easy to meet and depend on a single factor. Generally, "Very Cold-Cold-Cool" conditions prevail in the city until

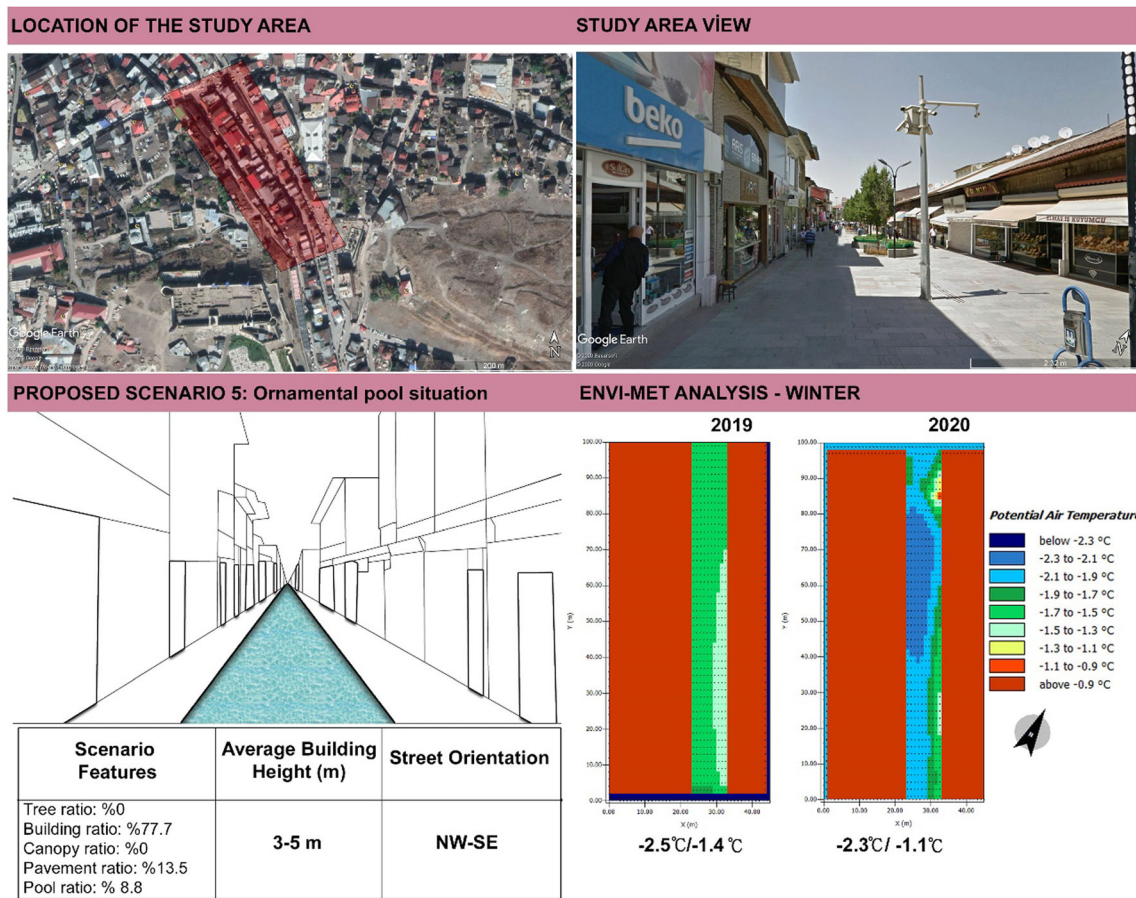
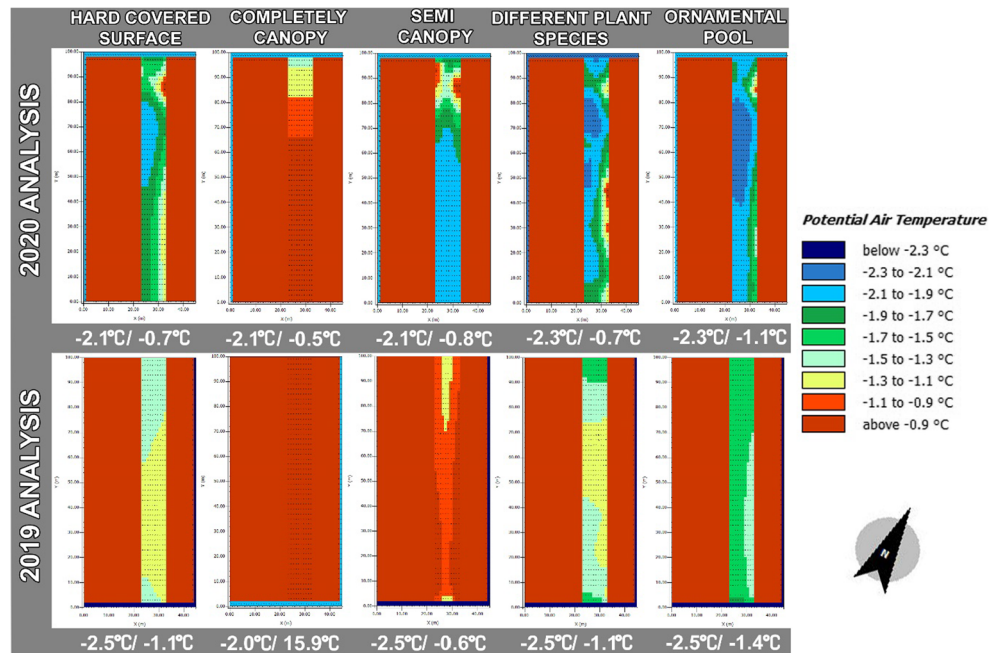


Fig. 14 Proposed scenario 5 (ornamental pool) perspective view

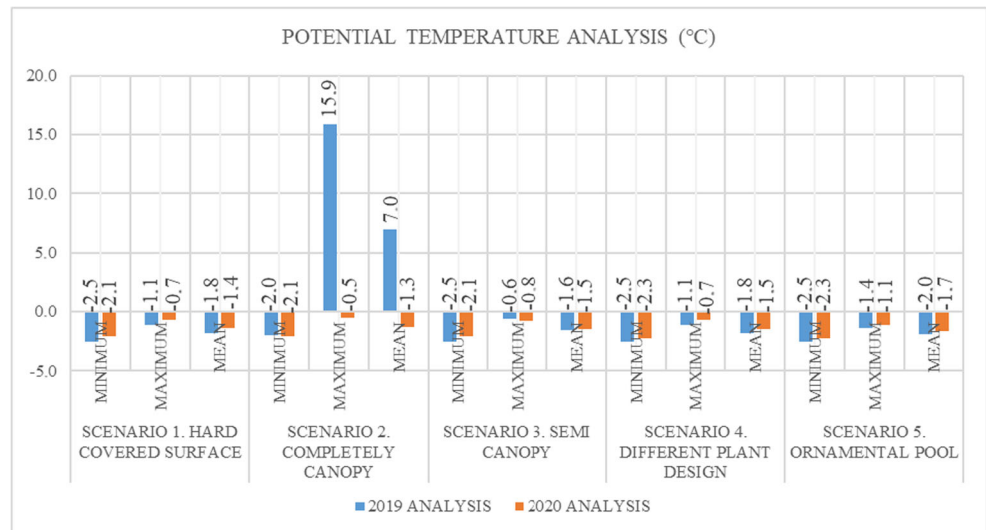
December–February and sometimes until March. It is important that this cold stress is improved by some design scenario. Many more scenarios need to be analyzed.

The water surface used in this study is a 15–20-cm ornamental pool. However, a water of this depth will probably freeze in Erzurum in winter. This scenario may be more

Fig. 15 ENVI-met analysis of scenarios created for February 25, 2019, and February 25, 2020 (scenario 2: this result was evaluated by ignoring the high maximum values)



**Fig. 16** Potential temperature analysis of scenarios (scenario 2: this result was evaluated by ignoring the high maximum values)



comfortable for the summer. However, it can be used as ice skating when it freezes in the winter months. Therefore, while preparing design scenarios, care should be taken to ensure that they can be used in all seasons. The average ENVI-met analysis of the scenario with water revealed that it was at least 0.4 °C cooler compared with that of the base scenario (hard covering). The use of water elements in pedestrian roads positively affects the psychology of individuals and also cools the space in summer (Du et al. 2016; Fung and Jim 2020; Xiong et al. 2020), and it reduces thermal comfort by making the area even colder in winter.

## Conclusion

Our thermal comfort analysis determined that the semi-open, semi-closed canopy design is more suitable for this street in winter. In this scenario, the openness is advantageous as it will positively affect ventilation and plant growth in the summer months. Water surfaces may be ideal to build small ornamental pools in this type of space, especially in summer, but the water will have to be turned off in winter. These venues can be adapted for ice skating in a controlled manner in the winter months. Thus, by create use area in the winter months, the vitality of the space will be enhanced.

The results helped identify appropriate landscape design scenarios and design strategies for the pedestrian street to create comfortable outdoor environments in a cold winter region. Street designs that will enable pedestrians to walk around comfortably in terms of thermal comfort are important. People working in the planning and design discipline should conduct even more research on this subject. Especially in urban renewal and transformation areas, better space designs should be made for people by increasing their thermal comfort. According to our analyses, the thermal comfort of the environment can be

improved when the microclimate data of the space is taken into account in landscape planning and design study. This is also vital for livable pedestrian-friendly road designs.

**Acknowledgements** This work was orally presented at the “ICEEE’2020 International Conference on Economics, Energy and Environment, Türkiye, 25- 27 Haziran 2020”. Authors present their special thanks to “Scientific and Technological Research Council of Turkey, TÜBİTAK under Project No: 2150627” and Turkish State Meteorological Service (MGM) for sharing their data free of charge.

**Authors’ contributions** S.Y. and B.E.M.: methodology; S.Y.: validation; S.Y., E.A.K., S.Y., and B.E.M.: formal analysis; E.A.K.: resources and introduction; S.Y. and E.A.K.: collected data; E.A.K. and S.Y.: data curation; S.Y., E.A.K., and B.E.M.: contributed data or analysis tools; S.Y., E.A.K., and B.E.M.: writing—original draft preparation; S.Y. and E.A.K.: writing—review and editing; S.Y. E.A.K., and I.S.: visualization; S.Y. and E.A.K.: supervision.

**Data availability** All data in this article will be available upon request. Legal permission is not required for the use and analysis of all data in this article.

## Compliance with ethical standards

**Competing interests** The authors declare that they have no conflict of interest.

**Ethical approval** Ethical approval is not required for this article.

**Consent to participate** No human or animal specimens were used in this work. The environment is not damaged.

**Consent to publish** All the authors agreed to publish the data in this journal.

## References

Abaas ZR (2020) Impact of development on Baghdad’s urban microclimate and human thermal comfort. *Alex Eng J* 59(1): 275–290

- Acero JA, Arrizabalaga J (2018) Evaluating the performance of ENVI-met model in diurnal cycles for different meteorological conditions. *Theor Appl Climatol* 131:455–469
- Algeciras JAR, Consuegra LG, Matzarakis A (2016) Spatial-temporal study on the effects of urban street configurations on human thermal comfort in the world heritage city of Camagüey-Cuba. *Build Environ* 101:85–101
- Bakarman MA, Chang JD (2015) The influence of height/width ratio on urban heat island in hot-arid climates. *Procedia Eng* 118:101–108
- Barakat A, Ayad H, El-Sayed Z (2017) Urban design in favor of human thermal comfort for hot arid climate using advanced simulation methods. *Alexandria Engineering Journal* 56(4):533–543
- Battista G, Carnielo E, De Lieto VR (2016) Thermal impact of a redeveloped area on localized urban microclimate: a case study in Rome. *Energy Build* 133:446–454. <https://doi.org/10.1016/j.enbuild.2016.10.004>
- Battista G, de Lieto VR, Zinzi M (2019) Assessment of urban overheating mitigation strategies in a square in Rome, Italy. *Sol Energy* 180:608–621
- Bendida M, Djellouli A, Hamidat D, Bouzit M (2019) Structure of the out-flows behind buildings and influence of the geometry of the streets on the out-flows. *J Mater Eng Struct* 6(3):375–382
- Blazejczyk K, Epstein Y, Jendritzky G, Staiger H, Tinz B (2012) Comparison of UTCI to selected thermal indices. *Int J Biometeorol* 56(3):515–535
- Bourbia F, Boucheriba F (2010) Impact of street design on urban microclimate for semi arid climate (Constantine). *Renew Energy* 35(2):343–347
- Bowler DE, Buyung-Ali L, Knight TM, Pullin AS (2010) Urban greening to cool towns and cities: a systematic review of the empirical evidence. *Landsc Urban Plan* 97(3):147–155
- Bruse M (2000) Anwendung von mikroskaligen Simulationsmodellen in der Stadtplanung. In: Bernhard L, Küger T (eds) *Simulation Raumbezogener Prozesse: Methoden Und Anwendung*. University of Münster
- Bruse, M., 2020. ENVI-met 4: a microscale urban climate model. <http://www.envi-met.info>. []
- Cao A, Li Q, Meng Q (2015) Effects of orientation of urban roads on the local thermal environment in Guangzhou city. *Procedia Eng* 121:2075–2082
- Chatzidimitriou A, Axarli K (2017) Street canyon geometry effects on microclimate and comfort: a case study in Thessaloniki. *Procedia Environ Sci* 38:643–650
- Chen L, Ng E, An X, Ren C, Lee M, Wang U, He Z (2012) Sky view factor analysis of street canyons and its implications for daytime intra-urban air temperature differentials in high-rise, high-density urban areas of Hong Kong: a GIS-based simulation approach. *Int J Climatol* 32(1):121–136
- Chen A, Shang C, Shao J, Zhang J, Huang H (2017) The application of iron-based technologies in uranium remediation: a review. *Sci Total Environ* 575:1291–1306
- Cheung PK, Jim CY (2018) Comparing the cooling effects of a tree and a concrete shelter using PET and UTCI. *Build Environ* 130:49–61
- Chun B, Guldmann JM (2014) Spatial statistical analysis and simulation of the urban heat island in high-density central cities. *Landsc Urban Plan* 125:76–88
- Coccolo S, Kämpf J, Mauree D, Scartezzini JL (2018) Cooling potential of greening in the urban environment, a step further towards practice. *Sustain Cities Soc* 38:543–559
- De Abreu-Harbach LV, Labaki LC, Matzarakis A (2015) Effect of tree planting design and tree species on human thermal comfort in the tropics. *Landsc Urban Plan* 138:99–109
- Dirksen M, Ronda RJ, Theeuwes NE, Pagani GA (2019) Sky view factor calculations and its application in urban heat island studies. *Urban Clim* 30:100498
- Du H, Song X, Jiang H, Kan Z, Wang Z, Cai Y (2016) Research on the cooling island effects of water body: a case study of Shanghai, China. *Ecol Indic* 67:31–38
- Erell E, Pearlmutter D, Boneh D, Kutiel PB (2014) Effect of high-albedo materials on pedestrian heat stress in urban street canyons. *Urban Clim* 10:367–386
- Foley JA, DeFries R, Asner GP, Barford C, Bonan G, Carpenter SR, Helkowski JH (2005) Global consequences of land use. *Science*, 309(5734), 570–574
- Fung CK, Jim CY (2020) Influence of blue infrastructure on lawn thermal microclimate in a subtropical green space. *Sustain Cities Soc* 52:101858
- Golany GS (1996) Urban design morphology and thermal performance. *Atmos Environ* 30(3):455–465
- Golasi I, Salata F, de Lieto VE, Coppi M, de Lieto VA (2016) Thermal perception in the mediterranean area: comparing the mediterranean outdoor comfort index (moci) to other outdoor thermal comfort indices. *Energies* 9(7):550
- Gómez-Baggethun E, Barton DN (2013) Classifying and valuing ecosystem services for urban planning. *Ecol Econ* 86:235–245
- Gulyás Á, Unger J, Matzarakis A (2006) Assessment of the microclimatic and human comfort conditions in a complex urban environment: modelling and measurements. *Build Environ* 41(12):1713–1722
- Gunawardena KR, Wells MJ, Kershaw T (2017) Utilising green and bluespace to mitigate urban heat island intensity. *Sci Total Environ* 584:1040–1055
- Höppe PR (1993) Heat balance modelling. *Experientia* 49(9):741–746
- Höppe P (1999) The physiological equivalent temperature—a universal index for the biometeorological assessment of the thermal environment. *Int J Biometeorol* 43(2):71–75
- Hu L, Wilhelmi OV, Uejio C (2019) Assessment of heat exposure in cities: combining the dynamics of temperature and population. *Sci Total Environ* 655:1–12
- Huang KT, Lin TP, Lien HC (2015) Investigating thermal comfort and user behaviors in outdoor spaces: a seasonal and spatial perspective. *Adv Meteorol* 423508. <https://doi.org/10.1155/2015/423508>
- Huang J, Li F, Zeng G, Liu W, Huang X, Xiao Z, He Y (2016) Integrating hierarchical bioavailability and population distribution into potential eco-risk assessment of heavy metals in road dust: a case study in Xiandao District, Changsha city, China. *Sci Total Environ* 541:969–976
- Hwang RL, Lin TP, Matzarakis A (2011) Seasonal effects of urban street shading on long-term outdoor thermal comfort. *Build Environ* 46(4):863–870
- Imran HM, Kala J, Ng AWM, Muthukumaran S (2019) Effectiveness of vegetated patches as Green Infrastructure in mitigating Urban Heat Island effects during a heatwave event in the city of Melbourne. *Weather Clim Extrem* 25:100217
- Irmak MA, Yilmaz S, Mutlu E, Yilmaz H (2018) Assessment of the effects of different tree species on urban microclimate. *Environ Sci Pollut Res* 25(16):15802–15822
- Jamei E, Rajagopalan P (2019) Effect of street design on pedestrian thermal comfort. *Archit Sci Rev* 62(2):92–111
- Köppen W (1918) *Klassifikation der Klimate nach Temperatur, Niederschlag und Jahresablauf* (Classification of climates according to temperature, precipitation and seasonal cycle). *Petermanns Geogr Mitt* 64:193–203
- Köppen W, Geiger R (1954) *Klima der Erde* (Climate of the earth), Wall Map 1, 16 Mill. Klett-Perthes, Gotha
- Krüger E, Pearlmutter D, Rasia F (2010) Evaluating the impact of canyon geometry and orientation on cooling loads in a high-mass building in a hot dry environment. *Appl Energy* 87(6):2068–2078
- Lee H, Mayer H, Schindler D (2014) Importance of 3-D radiant flux densities for outdoor human thermal comfort on clear-sky summer days in Freiburg, Southwest Germany. *Meteorol Z* 23(3):315–330

- Lee H, Mayer H, Kuttler W (2020) Impact of the spacing between tree crowns on the mitigation of daytime heat stress for pedestrians inside EW urban street canyons under Central European conditions. *Urban For Urban Green* 48:126558
- Li G, Ren Z, Zhan C (2020) Sky view factor-based correlation of landscape morphology and the thermal environment of street canyons: a case study of Harbin, China. *Build Environ* 169:106587
- Liu Z, Zheng S, Zhao L (2018) Evaluation of the ENVI-met vegetation model of four common tree species in a subtropical hot-humid area. *Atmosphere* 9(5):198. <https://doi.org/10.3390/atmos9050198>
- Ma X, Fukuda H, Zhou D, Wang M (2019) Study on outdoor thermal comfort of the commercial pedestrian block in hot-summer and cold-winter region of southern China—a case study of the Taizhou Old Block. *Tour Manag* 75:186–205
- Maniatis S, Nastos P.T, Moustris K, Polychroni I., Kamoutsis A (2020) Human thermal sensation over a mountainous area, revealed by the application of ANNs: the case of Ainos Mt., Kefalonia Island, Greece. *International Journal of Biometeorology*, <https://doi.org/10.1007/s00484-020-01993-y>, inpress
- Matzarakis A, Mayer H, Iziomon MG (1999) Applications of a universal thermal index: physiological equivalent temperature. *Int J Biometeorol* 43(2):76–84
- Mayer H, Höpfe P (1987) Thermal comfort of man in different urban environments. *Theor Appl Climatol* 38(1):43–49
- MGM (2020) Turkish State Meteorological Service (MGM) shared their data. <https://www.mgm.gov.tr/>
- Monam A, Rückert K (2013) The dependence of outdoor thermal comfort on urban layouts. *Universitätsverlag der TU Berlin*
- Morakinyo TE, Kong L, Lau KKL, Yuan C, Ng E (2017) A study on the impact of shadow-cast and tree species on in-canyon and neighborhood's thermal comfort. *Build Environ* 115:1–17
- Morakinyo TE, Lau KKL, Ren C, Ng E (2018) Performance of Hong Kong's common trees species for outdoor temperature regulation, thermal comfort and energy saving. *Build Environ* 137:157–170
- Mutlu E, Yilmaz S, Yilmaz H, Mutlu BE (2018) Analysis of urban settlement unit by ENVI-met according to different aspects in cold regions. 6th annual international Conference on Architecture and Civil Engineering (ACE 2018), oral presentation, 14-15 May 2018, Singapore
- Nastos PT, Polychroni ID (2016) Modeling and in situ measurements of biometeorological conditions in microenvironments within the Athens University Campus, Greece. *Int J Biometeorol* 60:1463–1479
- OECD Publishing, Organisation for Economic Co-operation and Development Staff (2012) Redefining urban: a new way to measure metropolitan areas. *Organ Econ Coop Dev*
- Öztürk MZ, Çetinkaya G, Aydın S (2017) Climate types of Turkey according to Köppen-Geiger climate classification. *J Geogr* 35:17–27
- Palme M, Lobato A, Carrasco C (2016) Quantitative analysis of factors contributing to urban heat island effect in cities of latin-American Pacific coast. *Procedia Eng* 169:199–206
- Park M, Hagishima A, Tanimoto J, Narita KI (2012) Effect of urban vegetation on outdoor thermal environment: field measurement at a scale model site. *Build Environ* 56:38–46
- Pearlmutter D, Berliner P, Shaviv E (2007) Integrated modeling of pedestrian energy exchange and thermal comfort in urban street canyons. *Build Environ* 42(6):2396–2409
- Perini K, Magliocco A (2014) Effects of vegetation, urban density, building height, and atmospheric conditions on local temperatures and thermal comfort. *Urban For Urban Green* 13(3):495–506
- Perini K, Chokhachian A, Auer T (2018) Green streets to enhance outdoor comfort. In *Nature based strategies for urban and building sustainability* (pp. 119-129). Butterworth-Heinemann
- Potchter O, Cohen P, Lin TP, Matzarakis A (2018) Outdoor human thermal perception in various climates: a comprehensive review of approaches, methods and quantification. *Sci Total Environ* 631:390–406
- Qaid A, Ossen DR (2015) Effect of asymmetrical street aspect ratios on microclimates in hot, humid regions. *Int J Biometeorol* 59(6):657–677
- Qaid A, Lamit HB, Ossen DR, Shahminan RNR (2016) Urban heat island and thermal comfort conditions at micro-climate scale in a tropical planned city. *Energy Build* 133:577–559
- Santamouris M, Haddad S, Saliari M, Vasilakopoulou K, Synnefa A, Paolini R, Fiorito F (2018) On the energy impact of urban heat island in Sydney: climate and energy potential of mitigation technologies. *Energy Build* 166:154–164
- Shareef S, Abu-Hijleh B (2020) The effect of building height diversity on outdoor microclimate conditions in hot climate. A case study of Dubai-UAE. *Urban Clim* 32:1–26
- Shishegar N (2013) Street design and urban microclimate: analyzing the effects of street geometry and orientation on airflow and solar access in urban canyons. *J Clean Energy Technol* 1(1)
- Smith K, Liu S, Liu Y, Guo S (2018) Can China reduce energy for water? A review of energy for urban water supply and wastewater treatment and suggestions for change. *Renew Sust Energ Rev* 91:41–58
- Sosa MB, Correa EN, Cantón MA (2017) Urban grid forms as a strategy for reducing heat island effects in arid cities. *Sustain Cities Soc* 32:547–556
- Taleb D, Abu-Hijleh B (2013) Urban heat islands: potential effect of organic and structured urban configurations on temperature variations in Dubai, UAE. *Renew Energy* 50:747–762
- Taleghani M, Kleerekoper L, Tenpierik M, van den Dobbelsteen A (2015) Outdoor thermal comfort within five different urban forms in the Netherlands. *Build Environ* 83:65–78
- Toy S, Yilmaz S (2010) Evaluation of urban- rural bioclimatic comfort differences over a ten – year period; in the sample of Erzincan city reconstructed after a heavy earthquake. *Atmósfera* 23(4):387–402
- Tsoka S, Tsikaloudaki A, Theodosiou T (2018) Analyzing the ENVI-met microclimate model's performance and assessing cool materials and urban vegetation applications—a review. *Sustain Cities Soc* 43:55–76
- Unger J (2009) Connection between urban heat island and sky view factor approximated by a software tool on a 3D urban database. *Int J Environ Pollut* 36(1–3):59–80
- Unger J, Skarbit N., Kovács A., Gál T. (2020). Comparison of regional and urban outdoor thermal stress conditions in heatwave and normal summer periods: a case study. *Urban Climate*,32, 100619, inpress
- Willmott CJ (1982) Some comments on the evaluation of model performance. *Bull Am Meteorol Soc* 63(11):1309–1313. <https://doi.org/10.1175/1520-0477>
- Xiao XD, Dong L, Yan H, Yang N, Xiong Y (2018) The influence of the spatial characteristics of urban green space on the urban heat island effect in Suzhou Industrial Park. *Sustain Cities Soc* 40:428–439
- Xiong Y, Zhang J, Xu X, Yan Y, Sun S, Liu S (2020) Strategies for improving the microclimate and thermal comfort of a classical Chinese garden in the hot-summer and cold-winter zone. *Energy Build* 109914
- Xu X, Sun S, Liu W, García EH, He L, Cai Q, Zhu J (2017) The cooling and energy saving effect of landscape design parameters of urban park in summer: a case of Beijing, China. *Energy Build* 149:91–100
- Xu M, Hong B, Jiang R, An L, Zhang T (2019) Outdoor thermal comfort of shaded spaces in an urban park in the cold region of China. *Build Environ* 155:408–420
- Yang SR, Lin TP (2016) An integrated outdoor spaces design procedure to relieve heat stress in hot and humid regions. *Build Environ* 99:149–160
- Yilmaz H, Yilmaz S, Yavaş M, Mutlu E, Koç A (2016) Climate-sensitive pavement Modelling for pedestrian ways. 4th international conference on countermeasures to urban Heat Island (UHI) 2016. *Procedia Eng* 169:408–415

- Yilmaz S, Mutlu E, Yilmaz H (2018a) Alternative scenarios for ecological urbanizations using ENVI-met model. *Environmental Science And Pollution Research*, 25(26), 26307–26321; Doi: <https://doi.org/10.1007/S11356-018-2590-1>
- Yilmaz S, Mutlu E, Yilmaz H (2018b) Quantification of thermal comfort based on different street orientation in winter months of Urban City Dadaşkent. Doi: <https://doi.org/10.17660/Actahortic.2018.1215.12>, Edsg. Pennisi, L. Cremonini, T. Georgiadis, F. Orsini, G.P. Gianquinto, Isbn: 978-94-62612-12-9, 2406-6168 (electronic) , *Acta Hortic*, 1215: 67–72
- Yilmaz S, Yilmaz H, Irmak MA, Kuzulugil AC, Koç A 2018c. Effects of urban *Pinus sylvestris* (L.) plantation sites on thermal comfort. DOI: <https://doi.org/10.17660/ActaHortic.2018.1215.6>, *Acta Hortic*. 1215, 39–44
- Yilmaz S, Irmak MA, Mutlu BE, Yilmaz Z (2019) Analysis of the effect of different exterior front claddings on thermal comfort in sustainable environment by ENVI-met: Atatürk University Campus. Oral presentation ID-A-USP-033, International Civil Engineering and Architecture Conference, ICEARC 19, 17-20 Apr., Trabzon/Turkey
- Yilmaz S, Mutlu BE, Aksu A, Mutlu E, Qaid A (2021) Street design scenarios using vegetation for sustainable thermal comfort in Erzurum, Turkey. *Environ Sci Pollut Res* 28(3):3672–3693. <https://doi.org/10.1007/s11356-020-10555-z>
- Yoloğlu A, Zorlu F (2020) Definition of rurality and rural areas in Turkey: a methodological trial. *J Soc Sci Inst Mersin Univ* 3(2): 145–176
- Zanon B, Verones S (2013) Climate change, urban energy and planning practices: Italian experiences of innovation in land management tools. *Land Use Policy* 32:343–355
- Zhang Y, Du X, Shi Y (2017) Effects of street canyon design on pedestrian thermal comfort in the hot-humid area of China. *Int J Biometeorol* 61(8):1421–1432
- Zhang L, Zhan Q, Lan Y (2018) Effects of the tree distribution and species on outdoor environment conditions in a hot summer and cold winter zone: a case study in Wuhan residential quarters. *Build Environ* 130:27–39
- Zhang Q, Xu D, Zhou D, Yang Y, Rogora A (2020) Associations between urban thermal environment and physical indicators based on meteorological data in Foshan City. *Sustain Cities Soc* 60:102288

**Publisher's note** Springer Nature remains neutral with regard to jurisdictional claims in published maps and institutional affiliations.